Docket 50-155

Report

Derivation of Floor Responses Reactor Building

524 235

63

7908070350

D'APPOLONIA

Project No. 78-161
June 78

D'APPOLONIA
CONSULTING ENGINEERS, INC.

Report

Derivation of Floor Responses Reactor Building

Big Rock Point Nuclear Power Plant Charlevoix, Michigan

NUS Corporation
Rockville, Maryland

524 236

Report

Derivation of Floor Responses Reactor Building

524 237

D'APPOLONIA

CERTIFICATE OF COMPLIANCE
REPORT
DERIVATION OF FLOOR RESPONSES
REACTOR BUILDING
BIG ROCK POINT NUCLEAR POWER PLANT
CHARLEVOIX, MICHIGAN

I have reviewed the subject report, dated June 1978, presenting the derivation of floor responses for the Reactor Building at the Big Rock Point Nuclear Power Plant. The analysis has been performed consistent with the criteria and design bases established by the Owner and the methods used in the analysis are in compliance with United States Nuclear Regulatory Commission regulations and good engineering practice.

Richard D. Ellison
Registered Professional Engineer
State of Michigan
Certificate No. 18089
June 22, 1978

524 238

D'APPOLONIA

TABLE OF CONTENTS

524 239

D'APPOLONIA

LIST OF TABLES

LIST OF FIGURES

524 240

LIST OF FIGURES
(Continued)

524 241

REPORT
DERIVATION OF FLOOR RESPONSES
REACTOR BUILDING
BIG ROCK POINT NUCLEAR POWER PLANT
CHARLEVOIX, MICHIGAN

1.0 INTRODUCTION

D'Appolonia Consulting Engineers, Inc. (D'Appolonia) is pleased to submit this report to NUS Corporation (NUS) as documentation of the derivation of floor responses at various locations in the Big Rock Point Nuclear Power Plant Reactor Building due to seismic motions at the base. It is our understanding that the floor time histories derived at the spent fuel pool location will be used by NUS in the analysis of the new high density fuel racks that will be added to the spent fuel pool.

In order to develop an accurate representation of the floor time histories of motions of the structure, a mathematical model of the reactor building as described in Section 3.0 was developed. All salient characteristics of the structure including soil-structure interaction effects were represented in this model.

As discussed in this report considerable engineering judgement was required to estimate the properties of the subsurface soils and rock which were used to derive the soil-structure interaction parameters for the model. The floor responses were finally developed by performing a linear transient dynamic analysis of the system with three simultaneous orthogonal earthquake excitations of the structure at its foundation level. The floor response spectra at the specified locations were then derived from the floor time histories obtained at their respective locations. Because of the uncertainties in the subsurface material properties, recommendations on the effects of variations in the soil compliance functions used in the model have been provided.

524 242

The results of the analyses are presented in this report with appropriate graphs and are discussed in Section 6.0.

This report describes the details of this study in the following order:

- Section 2.0 - Analytical Methodology
- Section 3.0 - Development of Mathematical Model
- Section 4.0 - Input Seismic Motion
- Section 5.0 - Dynamic Analysis
- Section 6.0 - Results of Analyses
- Section 7.0 - Summary

2.0 ANALYTICAL METHODOLOGY

2.1 BACKGROUND INFORMATION

The Big Rock Point Nuclear Power plant is located about four miles to the northeast of Charlevoix, Michigan near the shore of Lake Michigan. The plant was put into commission in the early 1960's and is owned and operated by Consumers Power Company, Jackson, Michigan. The proposed addition of high density fuel racks in the spent fuel pool of the Reactor Building requires development of floor time histories and their respective response spectra at this location. At the time of original design, the seismic design basis was a zero period ground acceleration equal to 0.05g. However, a horizontal zero period design ground acceleration of 0.12g has been specified by the Owner (Notes, March 9, 1978, meeting at Consumers Power Company offices) for the analysis of fuel racks at this plant.

Because NUS is performing a time-history analysis of the fuel racks, both the floor time histories and the floor response spectra are being submitted to NUS at the spent fuel pool location. In addition, as per the request of NUS, floor response spectra at two additional locations in the structure are being submitted for any future equipment analysis.

2.2 SITE CONDITIONS

The representative site subsurface profile was determined from the records of borings performed by Raymond Concrete Pile Company (Consumers Power Company, 1978a). In general, the site subsurface profile may be described as composed of approximately ten feet of sand, gravel and limestone fragments at the surface underlain by about 40 feet of medium dense to very dense glacial deposits termed "hardpan." The standard penetration resistance in this glacial till deposit varies from a minimum of about 19 blows/ft to a maximum of over 100 blows/ft. Underlying the till is a gray to black fossiliferous limestone with thin shale partings to a depth of at least several hundred feet. Based on an

524 244

examination of the core recovery percentage, approximately the upper 15 feet of the limestone is relatively highly weathered. The groundwater table is very close to the ground surface.

Figure 1 shows the site plan and the locations of the Boring Nos. 3 through 9 drilled by Raymond (Boring Nos. 1 and 2 were drilled more than 1,500 feet off to the northwest). A schematic representation of the subsurface profile along an east-west section (Section 1-1, Figure 1) through the Reactor Building foundation is shown in Figure 2.

2.3 STRUCTURAL ARRANGEMENT

The Reactor Building consists of a 3/4-inch thick steel containment sphere approximately 129 feet in diameter which encloses the reactor vessel and core, the new and spent fuel storage areas, the steam generating system and auxiliary equipment. The reinforced concrete foundation is in the shape of an inverted spherical dome approximately seven feet thick. Within the containment sphere, the major equipment and structural arrangement are as shown in Figures 3 and 4. The Reactor Building is classified as a Category I structure.

Structures adjacent to the Reactor Building, as shown in Figure 1, include the Turbine Building and the office building, while the screen well and pumphouse are some distance removed. Because these structures are separated and independent from the Reactor Building, no interaction between these structures and the Reactor Building was considered in the analysis.

524 245

2.4 ANALYSIS PROCEDURE

The primary purpose of this analysis is to derive the floor time histories of motion in the three component directions at the spent fuel pool floor of the Big Rock Point Plant. The development of the structural model of the Reactor Building is presented in detail in Section 3.0. To accurately determine the required floor time histories, a three-dimensional shear beam model of the reinforced concrete Reactor Building internal structure was developed from the structural drawings of the plant.

To preserve the effects of interaction between the steel shell and the enclosed structure, an equivalent single-mass stick model having the frequency properties of the spherical shell was developed and attached at the base of the structure. Because the structure is located on glacial till deposits underlain by limestone bedrock, a representation of the soil-structure interaction between the foundation and the soil was provided through lumped springs and dampers. The structural model so developed is shown in Figure 5.

A mode-frequency analysis of this model was first performed to obtain its frequencies and mode shapes as a check for consistency in the modelling. The structure was then excited at the base by an artificial earthquake time history input acting simultaneously along three normal directions. The artificial earthquake records used in the analysis were generated as part of this study and satisfy the general requirements of the United States Nuclear Regulatory Commission (USNRC) Regulatory Guide 1.60 (1973) and USNRC Standard Review Plan 3.7.1 (1975). The development of these records is described in detail in Section 4.0. The details of the dynamic analysis are presented in Section 5.0.

To conservatively account for the possible variation of the subsurface material properties, the mode-frequency analysis was repeated by using a lower bound and upper bound estimate of the soil compliance functions used in the analysis. For lower bound analysis, the soil spring stiffnesses were reduced by 50 percent, while for the upper bound analysis, the stiffnesses were increased by a factor of 1.5. The detailed recommendations for incorporation of this variation in soil-structure interaction parameters for floor equipment analyses are discussed in Section 5.2.2.

524 246

The ANSYS Computer Code (DeSalvo and Swanson, 1975) was used for all dynamic analyses in this study. The program is based on the finite element technique. The artificial time histories and the floor response spectra were generated by using computer programs developed by D'Appolonia.

3.0 DEVELOPMENT OF MATHEMATICAL MODEL

3.1 SUPERSTRUCTURE MODEL

The Reactor Building is a spherical steel containment structure enclosing a very rigid concrete internal structure which performs all structural support functions related to the normal operation of the Reactor. The spherical steel containment provides two functions: it is an enclosure against the effects of the weather and it prevents radioactive contamination of the atmosphere in the event of an accident. Only those salient features of the containment shell which affect the response of the internal structure have been modeled.

3.1.1 Idealization of Reactor Internals

The internal structure rises from a base elevation of 573 feet and is composed of the steam drum enclosure, the reactor enclosure and the spent fuel pool. This congregation of structures is modeled as a single stick with centroid locations dictated by the centroids of the major horizontal sections through the structure. The masses of all floors, walls, equipment and water are lumped at the appropriate nodal locations. This mathematical idealization of the Reactor Building (Figures 3 and 4) is diagrammed in Figure 5.

3.1.1.1 Stick Properties

Horizontal sections were cut through the structure at mid-point elevations between all lumped masses shown in Figure 5. Axial bending, shear and torsional properties about the section centroid were calculated for each section based on the size and geometric arrangement of walls at the cut sections. The centroidal location of the structure above the 630-foot elevation was located to be offset by 22.7 feet in the X-direction and 6.4 feet in the Y-direction with respect to the centroidal location of the structure below the 630-foot elevation. This shift in the centroidal location was modeled by extending a rigid link member from Node 4 to Node 3 (Figure 5). The rigid link member was assigned axial bending and torsional properties sufficiently high to guarantee its behavior as a rigid link. Furthermore, rigid links were also used between Node 7 and Node 11, Nodes 15 and 13 and Nodes 14 and 13 (Figure 5). Node 11 represents the location of the new high density fuel racks in the spent fuel pool area where floor time histories and the floor response spectra were generated. Node 13 represents the base of the containment shell, whereas Nodes 14 and 15 are translational and torsional coupling nodes for Nodes 8 and 9, respectively, having the same respective coordinate specifications. As explained in Section 3.1.2, the rigid link connections between Nodes 15 and 13 and Nodes 14 and 13 represent the translational interaction between the shell and the internal structure.

The member properties were input to the computer code ANSYS using the STIF4 three-dimensional beam element. The properties input are presented in Table 1.

TABLE 1
INTERNAL STRUCTURE MEMBER PROPERTIES

MEMBER NODES	AREA $(ft)^2$	I_x $(ft)^4 \times 10^5$	I_y $(ft)^4 \times 10^5$	J $(ft)^4 \times 10^5$	α_x	α_y
1-2	478	1.85	0.41	0.96	2.9	1.7
2-3	596	2.17	0.60	1.38	3.3	1.5
4-5	1,480	5.94	5.69	3.74	1.7	1.6
5-6	1,740	8.78	6.62	4.40	1.8	1.7
6-7	1,920	11.43	8.03	3.87	1.7	1.7
7-8	1,540	9.71	10.30	0.32	2.1	2.0
8-9	2,320	12.30	11.90	21.90	2.1	1.9

Where, I_x = bending moment of inertia about X-axis
I_y = bending moment of inertia about Y-axis
J = torsional moment of inertia about Z-axis
α_x = shape factor in X-direction
α_y = shape factor in Y-direction

NOTE: See Figure 5 for definition of members and coordinate axes.

524 248

3.1.1.2 Mass Properties

All masses of the structure were modeled as lumped masses located at their nearest nodal locations as shown in Figure 5. The structural mass included the floors at the elevations of the nodes and the walls having a height incorporating half the distance to the floor level above and below. The mass moments of inertia for bending and torsion of the walls and floors about the centroidal axes were also lumped at the nodal locations.

The equipment masses and mass inertias (Consumers Power Company, 1978b; NUS Corporation, 1978) were distributed at nodes as shown in Figure 6. The equipment masses were positioned at the nodes nearest to their actual locations with the reactor vessel and crane masses split between two nodes. Table 2 shows the total lumped masses and mass inertias distributed at Nodes 1 through 9.

TABLE 2

INTERNAL STRUCTURE LUMPED MASSES

NODE	MASS ($lb-sec^2/ft \times 10^4$)	I_{xx} ($lb-sec^2-ft \times 10^7$)	I_{yy} ($lb-sec^2-ft \times 10^7$)	I_{zz} ($lb-sec^2-ft \times 10^7$)
1	3.62	1.06	0.22	1.26
2	4.12	1.40	0.37	1.69
3	2.22	0.85	0.26	1.03
4	5.05	1.45	1.17	2.62
5	6.46	4.20	2.50	7.11
6	11.80	6.34	6.06	13.1
7	21.8	17.7	12.9	26.7
8	18.0	36.4	35.8	72.1
9	23.2	8.3	8.1	16.3

1

Where, I_{xx} = mass moment of inertia about X-axis

I_{yy} = mass moment of inertia about Y-axis

I_{zz} = mass moment of inertia about Z-axis

524 249

NOTE: See Figure 5 for definition of nodes and coordinate axes.

The sloshing forces generated by the water in the spent fuel pool were calculated using the method outlined by Epstein (1976). The stiffness values of the spring-mass systems representing sloshing were compared to the stiffness of the members to which they were attached and the comparison indicated that the sloshing springs were several orders of magnitude softer than their structural counterparts as indicated by the mass and frequency ratios between the spring-mass system and the structural members. The sloshing springs were, therefore, removed from the model (USNRC Standard Review Plan 3.7.2 [1975]) and the horizontal mass of the water in the spent fuel pool was divided between Nodes 5, 6 and 7. The total vertical mass of the water in the spent fuel pool was placed on Node 7 at the elevation of the pool floor (see Figure 6).

3.1.2 Containment Shell

The three-quarter-inch thick steel containment shell is attached to the massive concrete internal structure. Because the mass of the containment shell is only four percent of the mass of the internal structure, a modal analysis of the shell was performed using axisymmetric elements with non-axisymmetric loading capabilities to ascertain if any shell modal frequencies fell near dominant modal frequencies of the internal structure. Using guidelines for seismic coupling set out in the RDT Standard (1974), comparisons of the natural frequency ratios between the containment shell and internal structure were made for all modes. The frequency ratios in the horizontal and vertical directions were within the range requiring seismic coupling of the two structures. The ratio of mass between the two structures, though small, was not sufficient to warrant decoupling by RDT standards.

The shell was modeled as a three-dimensional beam element, STIF4, with a lumped mass at the vertical centroid location of the shell. The bending and axial properties of this three-dimensional beam were adjusted to provide the same single degree of freedom frequency characteristics of the shell in its first three modes of displacements in the X, Y and Z directions. The transient analysis results obtained for the shell, therefore, are not meant to reflect the actual response of the shell but properly incorporate the effect of the mass of the shell on the response of the internal structure.

The base of the containment shell at Elevation 584.5 feet is supported by the common foundation of the shell and internal structure. This foundation has already been accounted for in the properties of the member connecting Node 8 to Node 9 of the internal structure. For this reason, the shell base was connected to Node 8; further, due to the fact that the shell interacts with the soil springs and dampers, it was also attached to Node 9. Both connections were made using rigid links with coupling in torsional and three translational directions at Nodes 8 and 9. Coincident Nodes 8 and 13 and Nodes 9 and 15 were used to specify the required directional couplings between the shell and the internal structure. This insured that only the horizontal and vertical frequency effects of the shell would be felt by the internal structure.

3.1.3 Structural Damping

The structural damping for both steel and concrete were chosen based on USNRC Regulatory Guide 1.61 (1973) for a Safe Shutdown Earthquake (SSE) event. The regulatory guide specifies four percent damping for welded steel structures and seven percent damping for reinforced concrete. These damping ratios were used to calculate the Rayleigh damping factor, β, for input to the ANSYS computer code (DeSalvo and Swanson, 1975).

The β factor provides a linear damping as follows:

$$D = \frac{\beta\omega}{2} \qquad (3.1.1)$$

where:

D = damping ratio,

ω = predominant circular frequency of the structure, rad/sec.

The damping matrix [D] was then computed by the ANSYS code from the element stiffness matrix [K] as:

$$[D] = \beta[K] \qquad (3.1.2)$$

The frequency at which damping would match the regulatory guide values was chosen based on the dominant response frequencies of the internal and shell structures. These frequencies were determined for the internal structure and the steel containment through examination of relative ratios of mode coefficients for different modes of vibration of the whole structure; the mode coefficients, calculated as the product of modal participation factors and spectral displacement, represent the relative displacement potential of the structure in their respective modes.

3.2 FOUNDATION MODEL

The foundation of the Big Rock Point Reactor Building is an inverted spherical concrete dome approximately seven feet thick embedded in the soil. Because of the existence of sand drains around the base of the containment shell and construction joints in the outer foundation block, as shown in Figure 7, the ground surface for embedment purposes was chosen at Elevation 584.5 feet. The foundation has an average diameter of 92.0 feet at this elevation which is actually eight feet below plant grade.

To determine the soil-structure interaction parameters, the inverted dome foundation was treated as an equivalent circular disk foundation. The disk was given a radius that provided the same surface area in contact with the soil as the dome foundation and was embedded to a depth equal to the centroid elevation of the inverted dome (Elevation 573 feet). The equivalent disk foundation was then placed on an idealized soil profile to evaluate the soil compliance functions which represent the interaction between the foundation and the subsurface.

3.2.1 Evaluation of Elastic Properties of Subsurface Layers

The subsurface profile was developed from boring logs provided by Consumers Power Company (1978a). The borings were supervised by Raymond Concrete Pile Company in 1959 as part of the original foundation design of the plant. Each boring log contains a general description of the sampled and cored materials at different depths and includes information on soil penetration resistance in blows per foot for glacial till and percentage of core recovery for the limestone bedrock. A general profile under the Reactor Building, as shown in Figure 8, was developed from these boring logs (also refer to Figure 2). As shown in Figure 8, the equivalent foundation disk was modeled as being supported directly on a layer of glacial till of thickness 28 feet which is underlain by a 15-foot layer of weathered limestone followed by a layer of competent limestone considered to be bedrock.

The basis for subdividing the limestone into two layers was percent core recovery shown on the boring logs; weathered rock has core recovery <50 percent. Because the available subsurface data did not contain any direct data on the elastic properties of the limestone rock, an average elastic modulus of a very competent limestone was first estimated to be equal to 8×10^6 psi for data based on tests on a large number of limestone rock samples (Deere, et al., 1966). This value of elastic modulus was then reduced by about 50 percent for the competent limestone and by about 85 percent for the weathered limestone by assuming that the core recovery percentage is a direct function of Geomechanics classification rating and then using Kulhawy's (1978) relationship between strength reduction in rock versus the Geomechanics rating. These reductions account for both quality and mass effects in the rock present at the site, whereby rock quality was related to the recovery percentage. The elastic properties obtained in this manner thereby assigned to the weathered rock an elastic modulus approximately one-third the value of the elastic modulus of the more competent rock underlying it.

The elastic properties of the glacial till have a much more predominant effect on the soil-structure interaction parameters. Due to a lack of sufficient appropriate data on the elastic properties of the glacial till, best estimate elastic properties were used in the computation of the soil-structure interaction parameters; lower and upper bound values for the interaction parameters were also determined.

Using soil data on grain-size distribution and effective stress parameters provided by Consumers Power Company (1978c), empirical relations developed by Hardin (1973) for gravelly soils, and D'Appolonia's previous experience with glacial tills, a best estimate shear wave

524 253

velocity of 1,700 feet per second was postulated. The corresponding shear modulus, computed by using the relationship

$$G = \rho V_s^2 \qquad (3.2.1)$$

where,

G = shear modulus,

ρ = mass density, and

V_s = shear wave velocity,

was found to be approximately one-fifth of the shear modulus of the underlying weathered rock.

3.2.2 Soil-Structure Interaction Parameters

Using the shear moduli obtained above and the total mass moments of inertia of the reactor building, the equivalent spring constant and damping for each response mode (degree of freedom) of the foundation were calculated for the layered system. The static spring constants for a rigid circular footing resting on an equivalent elastic half-space may be calculated using the formulae given in Table 3, and damping values using the formulae given in Table 4. The technique developed by Christiano, et al. (1974) was used to reduce the layered medium to an equivalent elastic half-space for each mode. This technique is based on the assumption that within each layer of a multi-layered system, the strain energy is equal to that contained between the same elevations in a homogeneous medium having the same elastic modulus as the layer. For each static displacement mode, the strain energy in the layered medium is estimated by assuming a stress distribution equal to that incurred in a homogeneous elastic half-space. By equating the strain energy to external work, a single elastic spring for each mode, equivalent to the multiple spring system representing the various layers, may be obtained.

TABLE 3

SPRING CONSTANTS FOR RIGID CIRCULAR FOOTING RESTING ON ELASTIC HALF-SPACE[1]

MOTION	SPRING CONSTANT[2]	REFERENCE
Vertical	$K_z = \frac{4Gr_o}{1-\nu}$	Timoshenko & Goodier (1951)
Horizontal	$K_x = \frac{32(1-\nu)Gr_o}{7-8\nu}$	Bycroft (1956)
Rocking	$K_\psi = \frac{8Gr_o^3}{3(1-\nu)}$	Borowicka (1943)
Torsion	$K_\theta = \frac{16}{3} Gr_o^3$	Reissner & Sagoci (1944)

(1) Reference: Richart, Hall and Woods (1970)

(2) G = shear modulus of elastic half-space
ν = Poisson's ratio
r_o = equivalent radius

524 255

TABLE 4

DAMPING RATIOS FOR RIGID CIRCULAR FOOTING RESTING ON ELASTIC HALF-SPACE[1]

MODE OF VIBRATION	MASS (OR INERTIA) RATIO[2]	DAMPING RATIO D
Vertical	$B_z = \frac{(1-\nu)}{4} \frac{m}{\rho r_o^3}$	$D_z = \frac{0.425}{\sqrt{B_z}}$
Sliding	$B_x = \frac{(7-8\nu)}{32(1-\nu)} \frac{m}{\rho r_o^3}$	$D_x = \frac{0.288}{\sqrt{B_x}}$
Rocking	$B_\psi = \frac{3(1-\nu)}{8} \frac{I_\psi}{\rho r_o^5}$	$D_\psi = \frac{0.15}{(1+B_\psi)\sqrt{B_\psi}}$
Torsional	$B_\theta = \frac{I_\theta}{\rho r_o^5}$	$D_\theta = \frac{0.50}{1+2B_\theta}$

[1] Reference: Richart, Hall and Woods (1970)

[2] ν = Poisson's ratio
r_o = equivalent radius
ρ = mass density of soil
m = mass of foundation
I_ψ = rotational mass moment of inertia of foundation
I_θ = torsional mass moment of inertia of foundation

524 256

3.2.2.1 Frequency and Embedment Corrections of Soil Springs

The lumped spring constants calculated above were corrected for frequency and embedment effects. The frequency corrections account for the dynamic stiffness relationships for a soil-foundation system while the embedment corrections represent the stiffening effects of the soil due to confinement of the foundation.

Frequency Corrections - Neglecting the small coupling between the horizontal and rocking motions, the relationship between the force amplitudes and displacement amplitudes for a massless disk supported on a homogeneous elastic half-space may be defined as (Veletsos and Verbic, 1973 and Verbic and Veletsos, 1972):

$$P_j = Q_j u_j \tag{3.2.2}$$

where:

P_j represents the generalized force amplitudes,
u_j represents the generalized displacement amplitudes, and
Q_j is a complex-valued stiffness or impedance function of the form

$$Q_j = K_j \; [k_j(a_o, \nu) + ia_o c_j(a_o, \nu)] \tag{3.2.3}$$

The symbol K_j represents the static stiffness of the disk in j-direction and k_j and c_j are dimensionless functions of Poisson's ratio of the soil, ν, and the dimensionless frequency parameter

$$a_o = \omega r_o / V_s \tag{3.2.4}$$

where:

ω = angular frequency,
r_o = radius of the disk, and
V_s = the shear wave velocity.

524 257

In the equivalent spring-dashpot system representation of the supporting medium, k_j and c_j may be thought of as the dynamic variation of the stiffness and damping parameters, respectively, of the medium. Then the values of $K_j k_j$ represent the frequency-corrected values of spring constants and $K_j a_o c_j$ represent the frequency-related values of damping.

The values of functions k_j and c_j under dynamic loading conditions have been estimated by Verbic and Veletsos (1972) for all translational and rocking modes and by Veletsos and Nair (1973) for the translational mode. Curves of k_j and c_j as functions of a_o as given in the above references were used to compute these values. Because the damping coefficient has the most influence near resonance, the average of the k_j values calculated over the estimated building frequency range was used in the final computation of the frequency correction factors for the soil springs.

Embedment Corrections - The embedment correction factors in each displacement mode were obtained by considering the depth of embedment of the foundation models. The influence of embedment on the stiffness parameters for all modes of vibration has been evaluated using finite element techniques by Johnson, et al., 1974. The additional stiffening effects obtained from these embedment factors were reduced by a factor of two for conservatism (to account for excavation and any backfill effects).

3.2.2.2 Corrections to Soil Damping

The damping ratios calculated based on the equations of Table 2 represent radiation damping. Radiation damping is controlled by the geometry of the elastic half-space. For shallow soil layers overlying a stiff material, a portion of the radiation damping is lost by reflection of the radiating wave from the stiff layer. The amount of wave energy reflected is a function of the impedance, ρV_s, of each layer and is given by the following relation (Furrer, et al., 1973):

524 258

$$E.R. = \left[\frac{1 - \frac{\rho_1 V_1}{\rho_2 V_2}}{1 + \frac{\rho_1 V_1}{\rho_2 V_2}} \right] \times 100 \qquad (3.2.5)$$

where,

E.R. = percent of energy reflected

ρ_1 = mass density of the glacial till

ρ_2 = mass density of the weathered rock

V_1 = shear wave velocity in the glacial till

V_2 = shear wave velocity in the weathered rock

The radiation damping for each response mode was reduced by a factor equivalent to the reflected wave energy ratio. The radiation damping was then further reduced by a factor of one-half for conservatism.

The actual damping ratio is composed of radiation and material damping. The material damping is the result of internal friction losses within the soil structure. A value of five percent was assumed for all material damping and was added to the radiation damping in all modes.

The damping ratios were converted to damping constants for input to a damping matrix in the transient analysis. Frequency corrections for the lumped springs were quite small and, because the radiation damping component had already been conservatively reduced by one-half, such corrections were neglected for the damping. Furthermore, embedment corrections for the damping were conservatively not considered.

The final lumped spring and damping parameters used in the best estimate analyses are presented in Table 5.

524 259

TABLE 5

FREQUENCY AND EMBEDMENT CORRECTED
SOIL STRUCTURE INTERACTION PARAMETERS

MODE	LUMPED SPRING	LUMPED DAMPING
Vertical	2.27×10^{10} lb/ft	1.07×10^{8} lb-sec/ft
Horizontal	6.22×10^{9} lb/ft	3.54×10^{7} lb-sec/ft
Rocking	2.33×10^{13} lb-ft/rad	6.03×10^{10} lb-sec-ft/rad
Torsion	2.08×10^{13} lb-ft/rad	3.92×10^{10} lb-sec-ft/rad

524 260

4.0 INPUT SEISMIC MOTION

Artificial earthquake time histories (ATH's) were developed to simulate ground motions to which the structure is subjected during an earthquake. A time history is a series record of ground accelerations representing a seismic event. They were used in the analysis of the Reactor Building to induce base displacements for the model analysis.

Three ATH's were developed to represent ground motions in two normal horizontal directions and the vertical direction and having response spectra satisfying the general requirements of UNSRC Standard Review Plan Section 3.7.1. The peak zero period horizontal and vertical accelerations for these time histories were specified by Consumers Power Company to equal 0.12g and 0.08g, respectively (Notes, March 9, 1978 meeting at Consumers Power Company offices).

The time histories were derived to match smooth ground design response spectra (SGDRS) for horizontal and vertical earthquake motions. These ground response spectra are shown in Figure 9 for five percent critical damping. The horizontal SGDRS conform with the USNRC Regulatory Guide 1.60 (1973) recommendations. The vertical SGDRS follow the guidelines recommended by Newmark, et al. (1973) which were the basis for the USNRC Regulatory Guide 1.60. The duration of ground motion was determined to be equal to 12 seconds which adequately satisfies the total duration value determined using Bolt's (197?) procedure recommended by Standard Review Plan Section 2.5.2 (1975) D'Appolonia feels that the SGDRS selected for the horizontal and vertical directions provide the necessary conservatism for evaluating the effects of a postulated seismic event on the reactor internals at the Big Rock Point Nuclear Power Plant.

4.1 DEVELOPMENT OF ARTIFICIAL EARTHQUAKE TIME HISTORY

An existing ATH digitized at 0.01 second was revised by selective scaling to form one component of the horizontal earthquake record called the

North-South component record. The source time history was used to analytically excite single degree of freedom oscillators having natural frequencies ranging from 0.2 Hz to 49 Hz at five percent of critical damping. A record of peak response of each oscillator forms the response spectrum of the source time history.

The time history response spectrum was compared to the horizontal design response spectrum for five percent damping recommended by the USNRC in Regulatory Guide 1.60 (1973). Selected frequency components of the Fast Fourier Transform of the ATH were scaled to cause the time history response spectrum to approximate the design response spectrum. By an iterative procedure of scaling and matching, the original time history was altered so that its response spectrum matched the NRC spectrum to guidelines presented in USNRC Standard Review Plan 3.7.2 (1975). Baseline corrections were applied to the record in each iteration. Plots of the north-south horizontal acceleration time history and its associated response spectrum are plotted in Figure 9.

The vertical ATH was derived in the manner described above. Peak vertical acceleration was scaled to 0.08g or two-thirds peak horizontal acceleration. The vertical response spectrum was matched to the vertical design response spectrum recommended by Newmark, et al. (1973) as discussed earlier. The vertical acceleration time history and response spectrum are plotted in Figure 9.

The east-west component of the horizontal earthquake time history was derived directly from the north-south time history by putting a 0.16-second period of zero accelerations in front of the record and removing the same period of accelerations from the end. In this manner, statistical independence of the two horizontal components of excitation was achieved. The response spectra obtained matched the USNRC Regulatory Guide 1.60 (1973) design spectrum without further alteration.

To satisfy the requirements of the USNRC Standard Review Plan that all three earthquake components be [illegible]lated, the statistical independence of each of these three records with respect to the other two was calculated. The highest correlation coefficient between any two records was 0.070, which is below the maximum value of 0.16 recommended by Chen (1975).

4.2 DAMPING VALUES FOR WHICH RESPONSE SPECTRA WERE MATCHED

The recommended damping constants to be used for various components and materials when analyzing structural response are given by USNRC Regulatory Guide 1.61 (1973). Applicable values for this analysis are four percent for steel piping and equipment, and seven percent for reinforced concrete for the Safe Shutdown Earthquake. The time histories generated to match response spectra curves at five percent damping were used to compute oscillator response at four percent and seven percent damping. These response curves were compared to design response curves for four percent and seven percent damping. The time history accelerations were then scaled so that the response at four percent and seven percent damping enveloped the design response curves according to USNRC Standard Review Plan 3.7.1 (1975). The respective scale factors used for the north-south, east-west and vertical components so obtained were 1.03, 1.06 and 1.03.

524 263

5.0 DYNAMIC ANALYSIS

Two types of dynamic analysis were performed on the Reactor Building model: mode-frequency analysis and transient reduced linear analysis. Mode-frequency analysis was performed to obtain a stability check on the model and to examine the modal displacement characteristics of the structure at its natural frequencies of vibration. As explained previously in Section 3.1.3, such an analysis also provided the basis of computing the Rayleigh damping factor, β. Linear transient analysis was performed to obtain the floor time histories of motions at different locations of the structure from which the respective floor response spectra at the specified locations were obtained.

5.1 MODE-FREQUENCY ANALYSIS

The fixed base location of the structure was defined at Node 10 of the model (Figure 6) for the mode-frequency analysis of the structure. Node 10 was considered fixed against all translations and rotations. The natural frequencies of the structure obtained from this mode-frequency analysis are shown in Table 6. As may be seen in Table 6, the first frequency of the structure is approximately 4.1 Hertz. However, this frequency is a torsional frequency of the structure above Node 7, with all nodes below Node 7 remaining practically fixed. The next two frequencies of the structure, which occur at approximately 6.8 and 6.9 Hertz, are primarily due to the vibration of the representation of the steel containment shell in the X and Y directions, respectively. The first general frequencies of the internal structure in the X and Y directions occur at approximately 9.3 and 9.5 Hertz, respectively, corresponding to the fourth and fifth natural frequencies of the combined structure. The sixth and all higher modes of the structure comprise combined participation by the shell and the internals.

524 264

The results of the mode-frequency analysis indicate an active localized torsional mode occurring at a relatively low frequency level. Thus, in the reduced linear transient analysis, in addition to translational degrees of freedom, specification of torsional degrees of freedom at Nodes 4 through 9 were judged to be necessary. Furthermore, two additional mode-frequency analyses were performed using the upper and lower bound estimates on soil spring constants as explained in Section 5.2.2.

5.2 TRANSIENT DYNAMIC ANALYSIS

The reduced linear transient dynamic analysis feature of the ANSYS computer code was used to derive the floor time histories of motion at different elevations of the structure. In this procedure, by using the matrix condensation technique, the stiffness, mass and damping matrices of the structure are reduced by specifying active dynamic degrees of freedom at the various nodes of the structure. The dynamic degrees of freedom as used in the analysis are shown in Figure 10; all translational degrees of freedom at each node were specified to be active along with torsional degrees of freedom at Nodes 4 through 9 to account for the relatively low-frequency localized torsional mode of the structure as explained in Section 5.1.

All rotational motions at fixed base Node 10 were considered to be fixed and the displacement time-histories of the design earthquakes were specified at this node. The displacement time histories of motion of the three components of the earthquake were obtained by twice numerically integrating the acceleration time histories developed as per the procedure described in Section 4.0.

The transient dynamic solution was obtained by numerically integrating the equations of motion. The ANSYS computer code uses the Houbolt numerical scheme in the transient dynamic analysis in which the displacement is a cubic function and the acceleration is a linear function across the time interval of integration. The initial velocity in the analysis was assumed to be equal to zero. This integration procedure is unconditionally stable for all time steps. However, to minimize the numerical damping which is inherent in this type of integration procedure for large time steps of integration, a time interval of 0.005 second was used in this analysis.

524 265

As discussed above, the records of time histories were evaluated at 0.01 second intervals. Since the time interval of integration used in all time history analyses were 0.005 second, the acceleration records were interpolated using the Fast Fourier Transform (FFT) routine (Rabiner, et al., 1972). The 0.01 second records were first transformed into the frequency domain. The frequency domain record, centered at zero frequency thus obtained, was symmetrically expanded to twice its original size by adding zeros to each end of the frequency domain. The new record was transformed back into the time domain using the FFT routine and a representation of the time histories at 0.005 second was thus obtained automatically.

5.2.1 Evaluation of Floor Response

The floor displacement time histories were obtained directly from the results of transient dynamic analysis. The floor acceleration time histories were obtained by twice differentiating the floor displacement time histories. Plots of these time histories are described in Section 6.0.

The floor response spectra were obtained by using a D'Appolonia in-house program for which the floor time histories of motion along any particular direction generated by the ANSYS routine are input. The program develops the floor acceleration time histories from this input and then computes and plots the floor spectra. All floor responses were calculated separately for the three orthogonal directions X, Y and Z, respectively, at three damping values (2, 4 and 7 percent of the critical). The minimum and maximum frequencies considered in the computation were 0.2 Hertz and 50 Hertz. The frequency points chosen for computation of all spectra were sufficient in accordance with the criteria recommended in Table 1 of USNRC Regulatory Guide 1.122 (1976).

5.2.2 Effects of Parameter Variation on Structural Response

USNRC Standard Review Plan Section 3.7.2 (1975) requires that in the analysis of sub-systems of a structure consideration should be given to expected variations in structural properties, dampings, soil properties and soil-structure interaction parameters. Detailed data and specifications for structural properties and dampings are available for this structure.

524 266

The variation from the specified values of these two parameters may thus be considered to be negligible. However, the elastic properties of the subsurface materials used in the derivation of the soil springs were not based on direct field investigation results. Therefore, a parametric study on the effects of variation in the soil compliance functions was considered necessary and was carried out by assuming an upper bound and a lower bound estimate on the soil spring constants.

In this procedure, it was assumed that the derived soil spring constants may vary ± 50 percent with respect to the best estimate values under the actual field conditions. Therefore, two additional mode-frequency analyses were performed by multiplying the best estimate soil spring constants by 0.5 and 1.5 for lower bound and upper bound analyses, respectively. The structural frequencies obtained in these two analyses are shown in Table 6 along with the frequencies obtained from the analysis using the best estimate soil springs.

The total frequency variation, $\pm \Delta f_j$, in any mode j is then calculated using the relationship (USNRC Regulatory Guide 1.122 [1976]):

$$\Delta f_j = [(0.05 f_j)^2 + (\Delta f_j^{\,s})^2]^{1/2} \qquad (5.2.\ )$$

where,

f_j = structural frequency in mode j using best estimate soil spring constants

$\Delta f_j^{\,s}$ = frequency variation in mode j due to variation in soil spring constants

Based on an inspection of the floor response spectra, the predominant frequencies of the structure were observed to occur approximately below 18 Hertz. Thus, Δf_j in Equation (5.2.1) was calculated for all modes below 18 Hertz for both upper and lower bound frequencies. The maximum value of the $(\Delta f_j / f_j)$ ratio was found to be equal to 0.195. Therefore, it is recommended that a value of $\pm 0.195\ f_j$ be used by NUS for peak broadening in all floor response spectra obtained from this analysis.

524 267

For time-history analyses of equipment at the spent fuel pool location, it is recommended that upper and lower bound analyses be performed using time intervals given by (Tsai [1974]):

$$\Delta t' = \left[1 \pm \frac{\Delta f_i}{f_i}\right] \Delta t = K\ (\Delta t) \qquad (5.2.2)$$

where,

$\Delta t'$ = the modified time interval,

Δt = the time interval used in best estimate analyses = 0.005 second, and

$$K = \left[1 \pm \frac{\Delta f_i}{f_i}\right]$$

Following this procedure, the modified time intervals for upper and lower bound analyses are obtained as 4.025×10^{-3} and 5.975×10^{-3} seconds, respectively. Furthermore, it is to be noted that if floor displacement time-histories of motion are used by NUS in the analysis of the high density fuel racks, the diaplacement ordinates of floor motion should be multiplied by a factor K^2, that is, by 0.648 and 1.428 for upper and lower bound analyses, respectively.

The effects of such variation in time interval on the response spectra are shown as examples for Node 11 (spent fuel pool location) in Figures 13 through 15, for two percent damping, along X, Y and Z axes, respectively. As per request by NUS (telecon record of May 26, 1978), no peak broadening of the floor response spectra was performed by D'Appolonia.

524 268

TABLE 6

NATURAL FREQUENCIES OF REACTOR BUILDING
BIG ROCK POINT NUCLEAR POWER PLANT

MODE NO.	ANALYTICAL FREQUENCIES IN HERTZ		
	LOWER BOUND(1)	BEST ESTIMATE	UPPER BOUND(2)
1	4.03	4.08	4.10
2	6.07	6.77	6.95
3	6.19	6.87	7.04
4	8.36	9.27	9.89
5	8.47	9.50	10.22
6	14.24	17.55	18.47
7	14.84	18.25	19.31

(1) Best estimate soil springs were multiplied by 0.5 in this analysis.

(2) Best estimate soil springs were multiplied by 1.5 in this analysis.

524 269

6.0 RESULTS OF ANALYSES

Results of analyses are presented in the form of plots of time-histories and floor response spectra. As per request of NUS, such results are presented for Node 1 (El. 657.5 feet), Node 3 (El. 630 feet) and for Node 11 (spent fuel pool location). Both acceleration and displacement time-histories of floor motion along X, Y and Z directions at Node 11 are shown in Figure 11. Only acceleration time-histories of the other two nodes, Node 1 and Node 3, are shown in Figure 12.

The maximum accelerations at the spent fuel pool location (Node 11) along X, Y and Z directions are approximately 8, 7 and 4 ft/sec^2, respectively, (Figure 11) which correspond to 0.25g, 0.22g and 0.12g acceleration, respectively. Therefore, the amplification of zero period floor accelerations over the zero period input accelerations of 0.12g horizontal and 0.08g vertical are then given by 2.08, 1.83 and 1.5 along X, Y and Z directions, respectively, at Node 11.

The levels of accelerations obtained for Node 3 (El. 630 feet) are given by (Figure 12) 8.5, 9.5 and 5 ft/sec^2 or 0.26g, 0.30g and 0.16g, respectively for X, Y and Z directions, respectively. The corresponding amplification factors with respect to zero period input accelerations are then 2.2, 2.5 and 2.0, respectively.

Finally, the levels of accelerations along X, Y and Z directions obtained at the topmost Node 1 (El. 657.5 feet) are shown to be (Figure 12) 11.5, 11.5 and 5 ft/sec^2 or 0.36g, 0.35 and 0.16g respectively. The corresponding amplification factors with respect to zero period input acceleration are 3.0, 3.0 and 2.0, respectively.

Floor response spectra for Node 11 along X, Y and Z directions are shown respectively in Figures 13 through 15, for Node 3 in Figures 16 through 18 and for Node 1 in Figures 19 through 21. In each of these figures, the response spectra are shown for three dampings - 2, 5 and 7 percent

524 270

of the critical. In addition, Figures 13 through 15 depict the effects of soil spring parameter variation as discussed in Section 5.2.2. The effects of such variation have been shown as examples for Node 11 along the X, Y and Z axes only for two percent of the critical damping.

524 271

7.0 SUMMARY

An analytic model was prepared for the Reactor Building of the Big Rock Point Nuclear Power Plant. The dynamic response of the model has been determined for base excitations resulting from three earthquake artificial time histories of motion in three orthogonal directions. The floor time histories of motion at three nodes of the model, including that representing the spent fuel pool location, have been computed from this analysis and the associated floor response spectra have been derived. The effects on the mode-frequency response of varying the soil spring constants have been computed, and recommendations are presented for proper consideration of these effects on the equipment analyses to be performed by NUS.

Respectfully submitted,

Satyananda Chakrabarti
S. Chakrabarti

Alan D. Husak
A. D. Husak

SC:ADH:ggo
Project No. 78-161
June, 1978

524 272

LIST OF REFERENCES

524 273

LIST OF REFERENCES

Bolt, B. A., 1973, "Duration of Strong Ground Motion," Proceedings of the Fifth World Conference on Earthquake Engineering.

Chen, C., 1975, "Definition of Statistically Independent Time Histories," Technical Note, Journal of the Structural Division, American Society of Civil Engineers, February.

Christiano, P. P., P. C. Rizzo and S. J. Jarecki, 1974, "Compliances of Layered Elastic Systems," Proceedings of the Institution of Civil Engineers, London, December.

Consumers Power Company, 1978a, Test Boring Report, Raymond Concrete Pile Company, Big Rock Point Site, February 1960.

Consumers Power Company, 1978b, "Big Rock Point Spent Fuel Racks - Components Weights," Internal Correspondence BRG18-78, Consumers Power Company Letter of Transmittal No. 5803-037, May 18.

Consumers Power Company, 1978c, Soil Report, Big Rock Point Plant, Charlevoix, Michigan, Soil Testing Services, Inc., March 1960.

Deere D. and R. Miller, 1966, "Engineering Classification and Index Properties for Intact Rock," Technical Report No. AFWL-TR-65-116, Air Force Weapons Lab., Kirkland Air Force Base, New Mexico.

DeSalvo, G. J. and J. A. Swanson, 1975, ANSYS - Engineering Analysis User's Manual, Swanson Analysis Systems, Elizabeth, Pennsylvania.

Epstein, H. I., 1976, "Seismic Design of Liquid Storage Tanks," Journal of the Structural Division, American Society of Civil Engineers, September.

Furrer, H., K. Gaehler, J. Jemielewski and J. R. Hall, Jr., 1973, "Soil Amplification and Soil-Structure Interation Study for a Nuclear Power Plant in Switzerland," Structural Mechanics in Reactor Technology, 2nd International Conference, Vol. 6B, September.

Hardin, B., 1973, "Shear Modulus of Gravels," Soil Mechanics Series No. 16, University of Kentucky, Kentucky.

Johnson, G. R., P. P. Christiano and H. I. Epstein, 1976, "Stiffness Coefficients for Embedded Foundations," Proceedings of the ASCE Power Division Specialty Conference, Boulder, Colorado, August.

Kulhawy, F. H., 1978, "Geomechanical Model for Rock Foundation Settlement," Journal of Geotechnical Engineering Division, American Society of Civil Engineers, February.

524 274

LIST OF REFERENCES
(Continued)

Newmark, N. M., J. A. Blume and K. K. Kapur, 1973, "Seismic Design Spectra for Nuclear Power Plants," Journal of the Power Division, American Society of Civil Engineers, November.

NUS Corporation, 1978, "Letter of Transmittal, Estimated Weights of Fuel Storage Rocks," May 26, 1978.

Notes on March 9, 1978, Meeting at Consumers Power Company with NUS, Consumers Power and D'Appolonia.

Rabiner, R. L., B. Gold and C. A. McGonegal, 1972, "An Approach to the Approximation Problem for Nonrecursive Digital Filters," Digital Signal Processing, R. L. Rabiner and C. M. Rader, eds., IEEE Press. New York.

Richart, F. E., Jr., J. R. Hall, Jr., and R. D. Woods, 1970, Vibration of Soils and Foundations, Prentice-Hall, Inc., Englewood Cliffs, New Jersey.

RDT Standard, 1974, "Seismic Requirements for Design of Nuclear Power Plants and Test Facilities," Division of Reactor Research and Development, U. S. Atomic Energy Commission, January.

Telecon Record of May 26, 1978 between D'Appolonia and NUS.

Tsai, N. C., 1969, "Transformation of Time Axes of Accelerograms," Journal of Engineering Mechanics Division, American Society of Civil Engineers, June.

USNRC Regulatory Guide 1.60, 1973, "Design Response Spectra for Seismic Design of Nuclear Power Plants," Directorate of Regulatory Standards, Rev. 1.

USNRC Regulatory Guide 1.61, 1973, "Damping Values for Seismic Design of Nuclear Power Plants," Directorate of Regulatory Standards, U. S. Atomic Energy Commission, October.

USNRC Regulatory Guide 1.122, 1976, "Development of Floor Design Response Spectra for Seismic Design of Floor Supported Equipment in Components," Office of Standards Development, U. S. Nuclear Regulatory Commission, September.

USNRC Standard Review Plan 2.5.2, 1975, "Vibratory Ground Motion," Office of Nuclear Reactor Regulation, U. S. Nuclear Regulatory Commission.

USNRC Standard Review Plan 3.7.1, 1975, "Seismic Input," Office of Nuclear Reactor Regulation, U. S. Nuclear Regulatory Commission.

524 275

LIST OF REFERENCES
(Continued)

USNRC Standard Review Plan 3.7.2, 1975, "Seismic System Analysis," Office of Nuclear Reactor Regulation, U. S. Nuclear Regulatory Commission, June.

Veletsos, A. S. and V. V. D. Nair, 1973, Torsional Vibration of Foundations, Structural Research at Rice, Report No. 19, Rice University, Houston, June.

Verbic, B. and A. S. Veletsos, 1972, Impulse Response Functions of Elastic Foundation, Structural Research at Rice, Report No. 15, Rice University, Houston.

Veletsos, A. S. and B. Verbic, 1973, "Vibration of Viscoelastic Foundations," Earthquake Engineering and Structural Dynamics, Vol. 2.

524 276

FIGURES

524 277

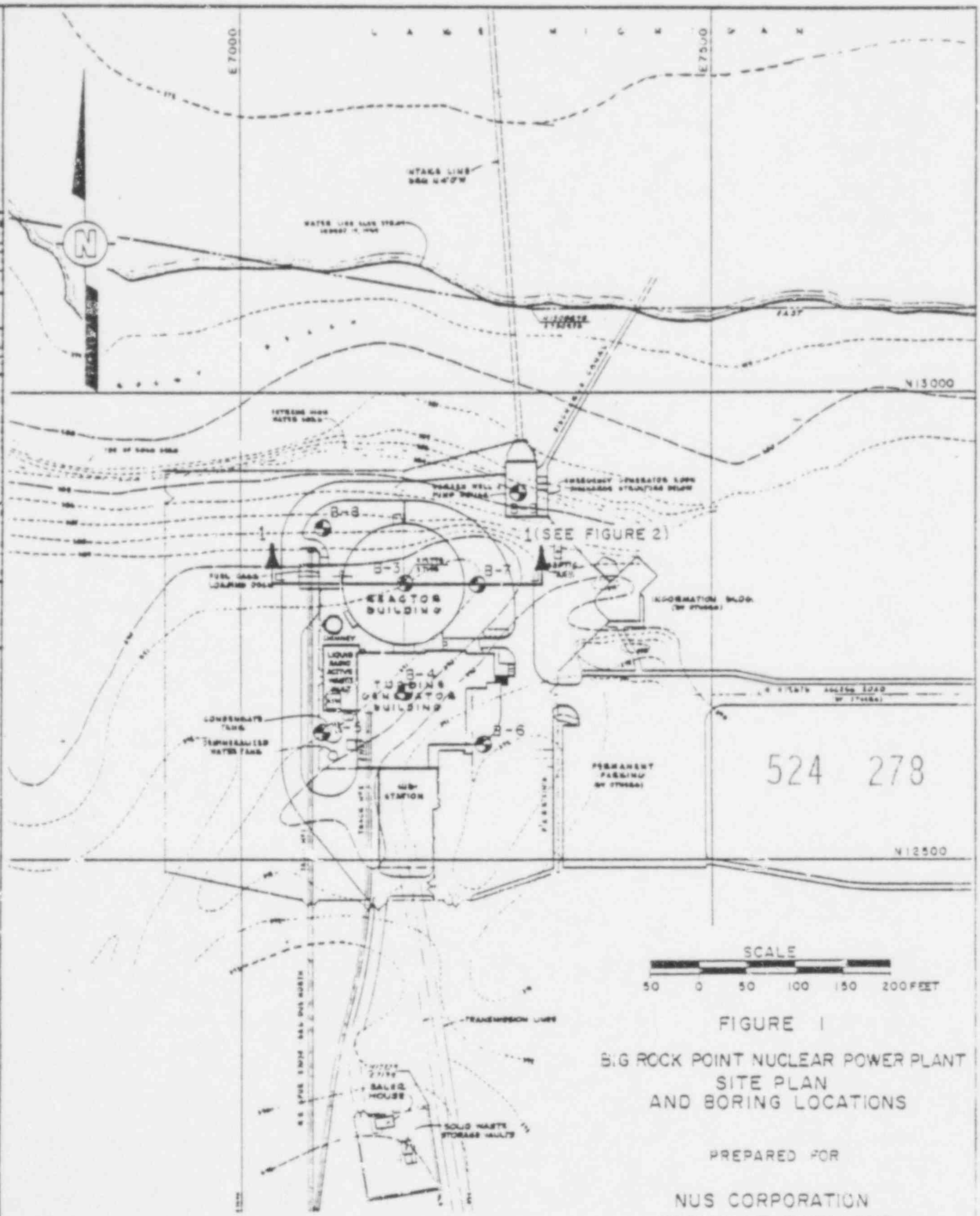

FIGURE 1

BIG ROCK POINT NUCLEAR POWER PLANT
SITE PLAN
AND BORING LOCATIONS

PREPARED FOR

NUS CORPORATION
ROCKVILLE, MARYLAND

DRAWN BY	ACS	5-19-78	DRAWING NUMBER 78-161-A2
CHECKED BY	SC	JUN 27 78	
APPROVED BY	APH	6/27/78	

REFERENCE:
BECHTEL DWGS 3159 C-2 REV. 1 (NEW DWG. NO. 0740G2002 REV. B) AND 3159 C-3 REV B

D'APPOLONIA

POOR ORIGINAL

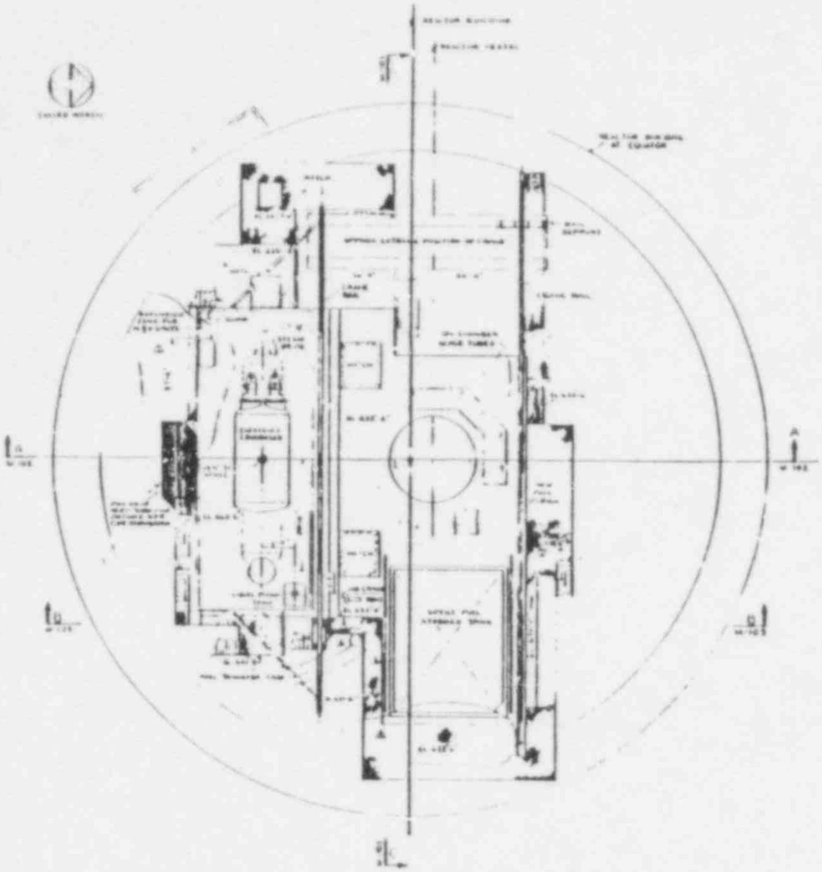

KEY PLAN
BELOW EL 674'-0"

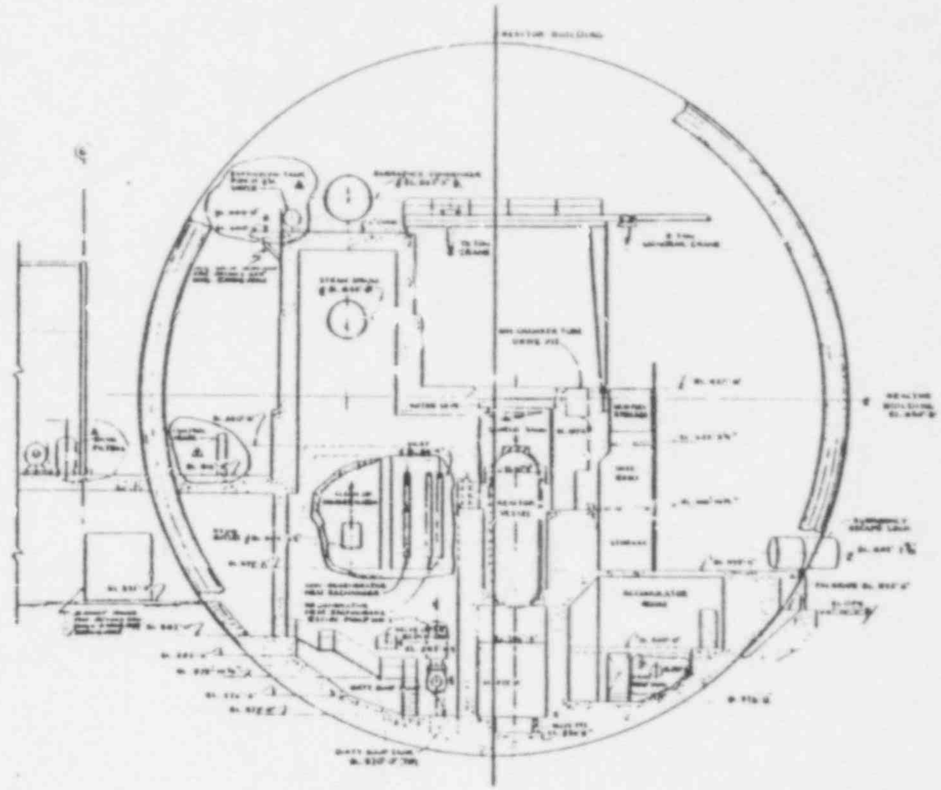

SECTION A-A

524 279

FIGURE 3

BIG ROCK POINT NUCLEAR POWER PLANT
STRUCTURAL ARRANGEMENT
REACTOR BUILDING
STRUCTURES AND EQUIPMENT
KEY PLAN AND SECTION A-A

PREPARED FOR

NUS CORPORATION
ROCKVILLE, MARYLAND

DAPPOLONIA

GRAPHIC SCALE
10 0 10 20 30 FEET

REFERENCE:
BECHTEL DWGS 3159-M-102 REV C(NEW DWG NO 0740640021) AND 3159-M-104 REV B(NEW DWG NO 0740640104)

DRAWING NUMBER 78-161-B2

POOR ORIGINAL

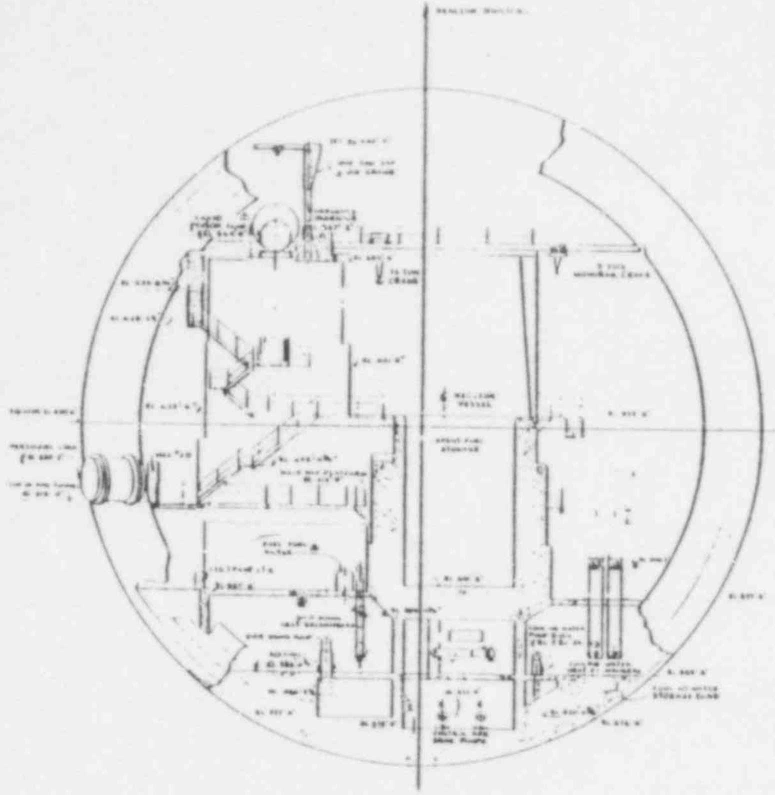

SECTION B-B

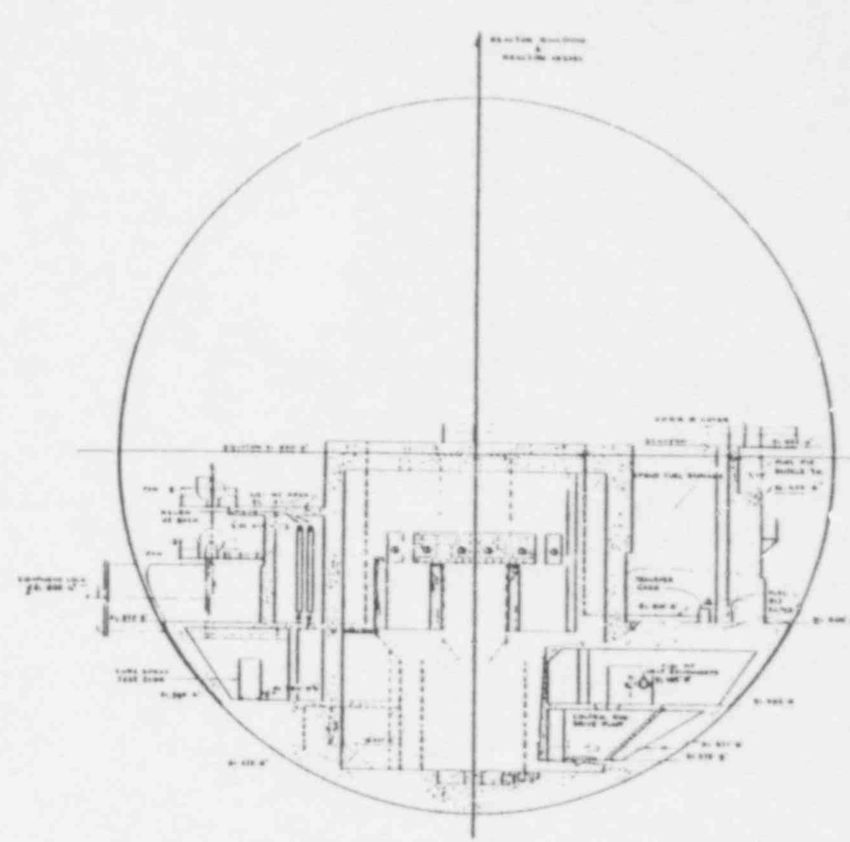

SECTION C-C

524 280

FIGURE 4

BIG ROCK POINT NUCLEAR POWER PLANT
STRUCTURAL ARRANGEMENT
REACTOR BUILDING
STRUCTURES AND EQUIPMENT
SECTIONS B-B AND C-C

PREPARED FOR

NUS CORPORATION
ROCKVILLE, MARYLAND

GRAPHIC SCALE

10 0 10 20 30 FEET

REFERENCE
BECHTEL DWG 3159 M 103 REV 2 (NEW DWG NO 0740G40103 REV A)

D'APPOLONIA

DRAWING NUMBER 76-161-B3

DRAWN BY	CHECKED BY	APPROVED BY	DRAWING NUMBER
ACS 5-22-78	SC JUN 27 78	ADH 6/27/78	78-161-A3

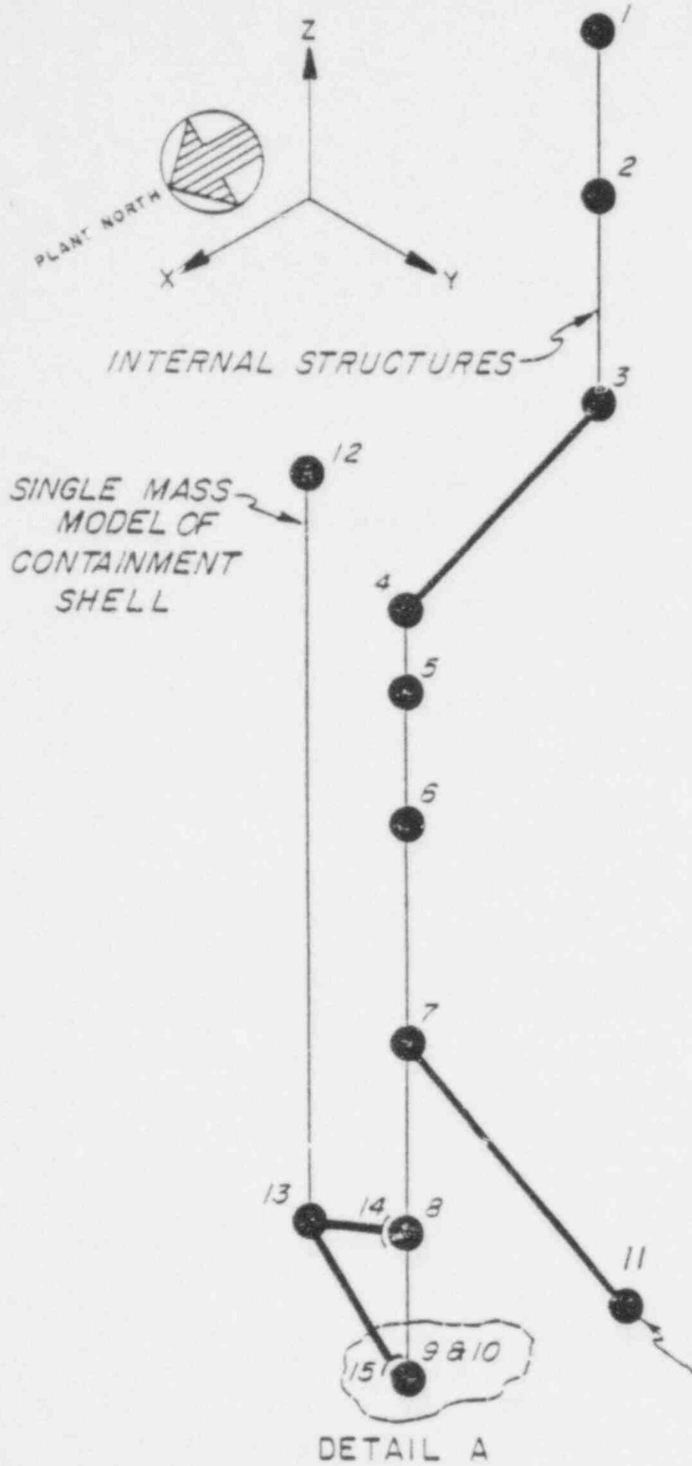

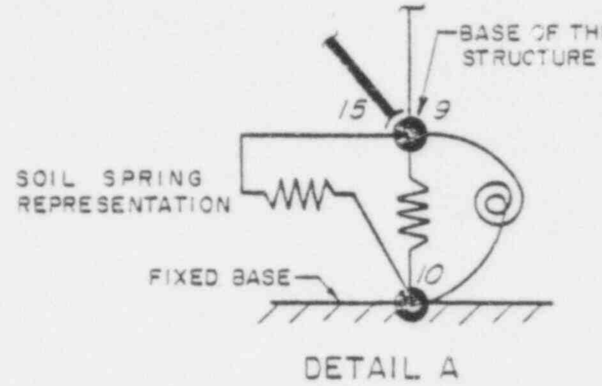

DETAIL A

NODAL LOCATIONS

NODE	X (FT)	Y (FT)	Z (FT)
1	-26.0	-1.4	657.5
2	-26.0	-1.4	645.5
3	-26.0	-1.4	623.0
4	-3.3	5.0	630.0
5	-3.3	5.0	624.0
6	-3.3	5.0	614.5
7	-3.3	5.0	598.5
8	-3.3	5.0	584.5
9	-3.3	5.0	573.0
10	-3.3	5.0	573.0
11	7.0	33.0	598.5
12	0.0	0.0	639.8
13	0.0	0.0	584.5
14	-3.3	5.0	584.5
15	-3.3	5.0	573.0

LEGEND:

- LUMPED MASS
- NODES COUPLED IN ALL THREE TRANSLATIONAL DIRECTIONS AND IN ROTATION ABOUT Z AXIS
- RIGID LINK
- 5 NODE NUMBER

FIGURE 5

BIG ROCK POINT NUCLEAR POWER PLANT
MATHEMATICAL MODEL

PREPARED FOR

NUS CORPORATION
ROCKVILLE, MARYLAND

D'APPOLONIA

524 281

POOR ORIGINAL

DRAWN BY	JCS 2-22-78	CHECKED BY	SC JUN 27 78	APPROVED BY	ADH	DRAWING NUMBER	78-161-B5

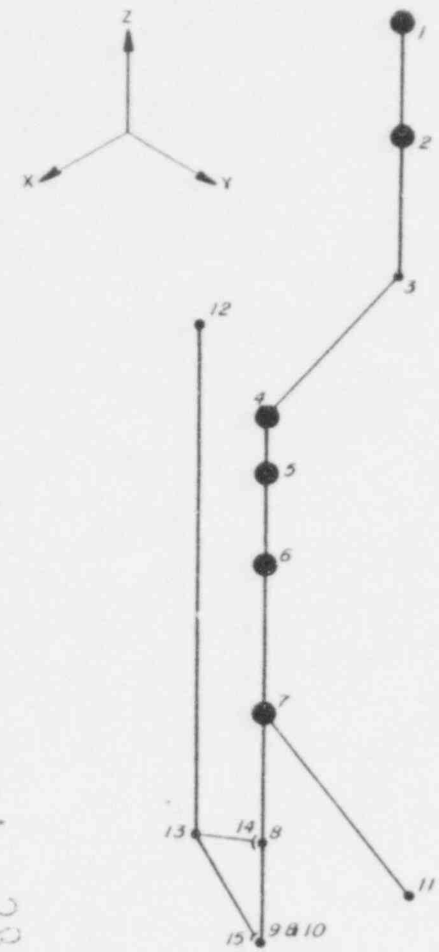

POOR ORIGINAL

524 282

EQUIPMENT MASSES

NODE	MASS (LB.-SEC^2/FT.)	DESCRIPTION
1	3,100	EMERGENCY CONDENSER AND ONE-HALF OF CRANE
2	7,000	STEAM DRUM
4	2,200	ONE-HALF OF CRANE
6	5,600	ONE-HALF OF REACTOR
7	13,950	ONE-HALF OF REACTOR AND SPENT FUEL POOL RACK

SPENT FUEL POOL WATER MASSES

NODE	MASS (LB-SEC^2/FT.)	
	HORIZONTAL	VERTICAL
5	11,360	NONE
6	11,290	NONE
7	6,550	29,200

LEGEND:

● LUMPED EQUIPMENT AND WATER MASSES

⊢● NODES COUPLED IN ALL THREE TRANSLATIONAL DIRECTIONS AND IN ROTATION ABOUT Z AXIS

5 NODE NUMBER

REVISION 1 UNITS CORRECTED
DRAWN BY: DAB 10-31-78
CHECKED BY: SC 11/1/78
APPROVED BY: ADH 11/1/78

FIGURE 6

BIG ROCK POINT NUCLEAR POWER PLANT
DISPOSITION OF EQUIPMENT AND WATER MASSES

PREPARED FOR

NUS CORPORATION
ROCKVILLE, MARYLAND

D'APPOLONIA

POOR ORIGINAL

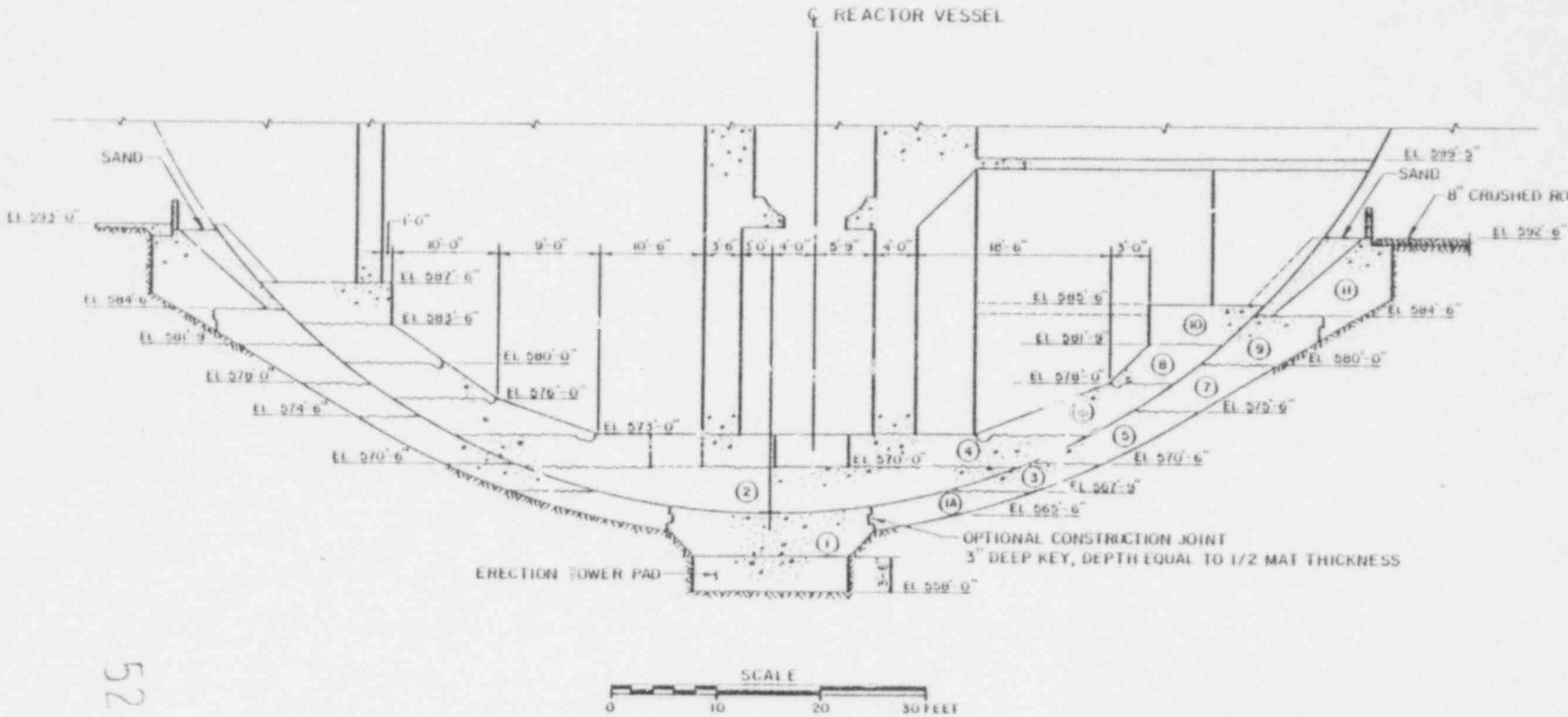

524 283

FIGURE 7

BIG ROCK POINT NUCLEAR POWERPLANT
REACTOR BUILDING
FOUNDATION CROSS-SECTION

PREPARED FOR

NUS CORPORATION
ROCKVILLE, MARYLAND

REFERENCE:
BECHTEL DRAWING NO. C 152
(NEW DRAWING NO 20 REV. A)

DAPPOLONIA

ELEVATION (FT)	SOIL PROFILE [1]	SHEAR MODULUS (PSI)	POISSON'S RATIO	UNIT WEIGHT [2] (PCF)
580	EQUIVALENT DISK FOUNDATION BOTTOM ELEVATION 573 FEET			
570 560 550	GLACIAL TILL	100,000	0.43	160
545 540	WEATHERED LIMESTONE	492,360	0.35	140
530 520 510 500	COMPETENT LIMESTONE	1,659,720	0.35	140

NOTE: NORMAL WATER TABLE ELEVATION 580 FT.

REFERENCES:

(1) CONSUMERS POWER COMPANY, (1978a).

(2) CONSUMERS POWER COMPANY, (1978c).

524 284

FIGURE 8

BIG ROCK POINT NUCLEAR POWER PLANT
ANALYTICAL SUB-SURFACE PROFILE

PREPARED FOR

NUS CORPORATION
ROCKVILLE, MARYLAND

D'APPOLONIA

DRAWN BY	T E J 5-17-78	CHECKED BY	SC JUN 27 78	APPROVED BY	ADH 6/27/78	DRAWING NUMBER	78-161-A1

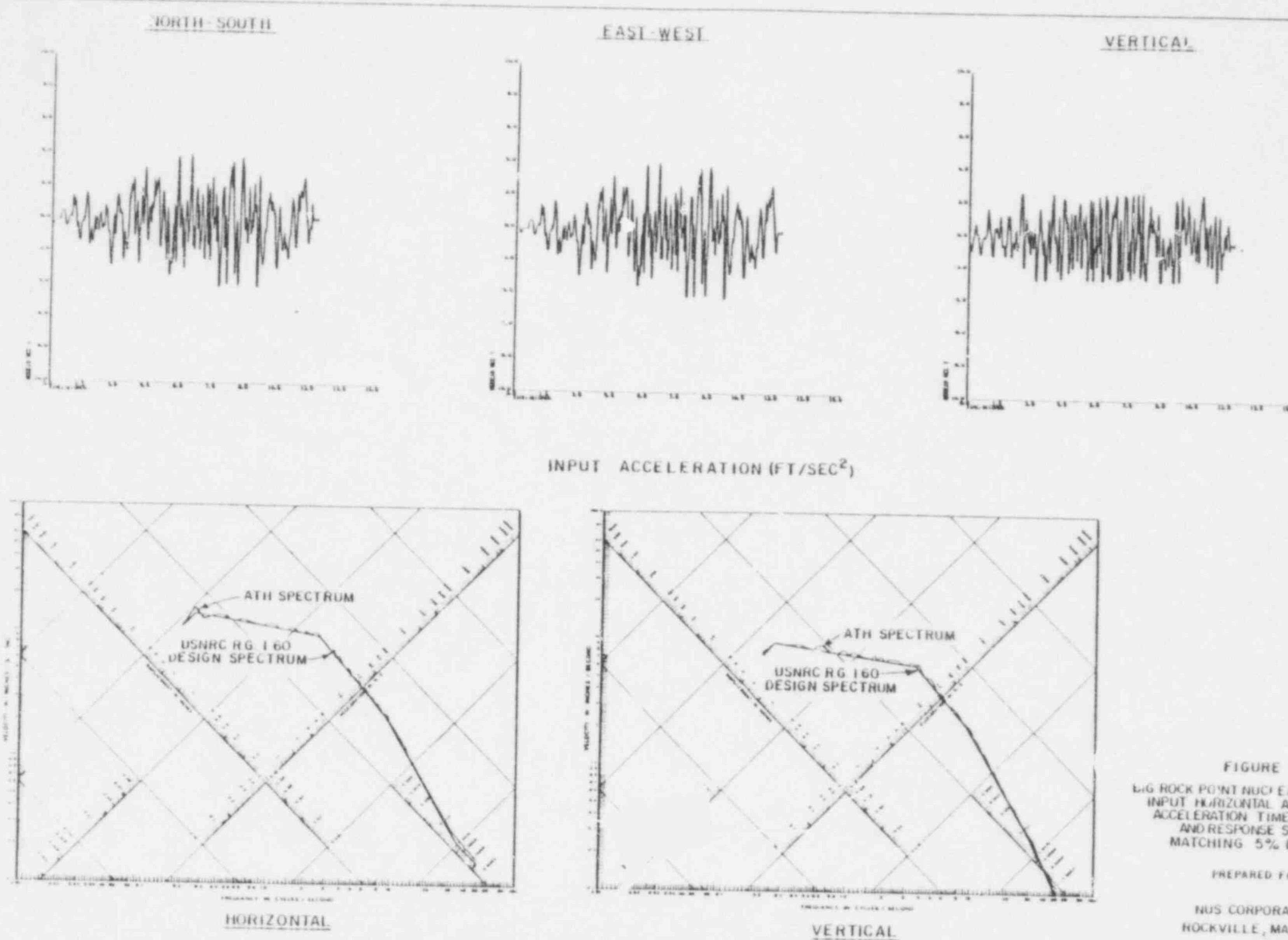

FIGURE 9

BIG ROCK POINT NUCLEAR POWER PLANT
INPUT HORIZONTAL AND VERTICAL
ACCELERATION TIME-HISTORIES
AND RESPONSE SPECTRA
MATCHING 5% DAMPING

PREPARED FOR

NUS CORPORATION
ROCKVILLE, MARYLAND

D'APPOLONIA

POOR ORIGINAL

524 285

DRAWN BY	CHECKED BY	APPROVED BY		DRAWING NUMBER
MEL 6-13-78	SC	ADH	JUN 27 78 6/27/78	78-161-A4

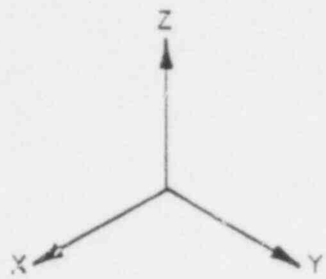

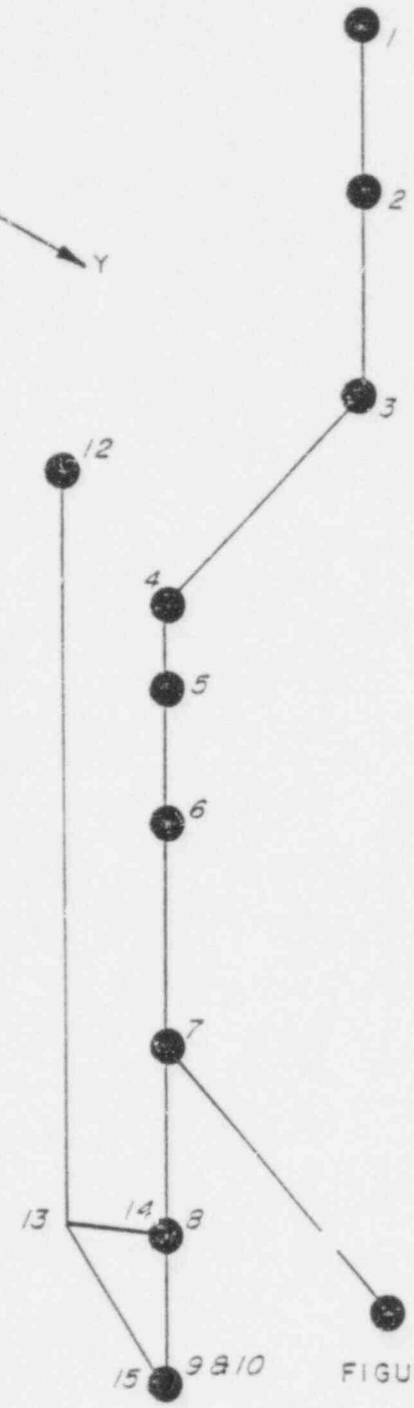

LIST OF DYNAMIC DEGREES OF FREEDOM

NODES	DDOF
1 THROUGH 3	UX, UY, UZ
10 THROUGH 12	UX, UY, UZ
4 THROUGH 9	UX, UY, UZ, ROTZ

FIGURE 10

BIG ROCK POINT NUCLEAR POWER PLANT
DYNAMIC
DEGREES OF FREEDOM

PREPARED FOR

NUS CORPORATION
ROCKVILLE, MARYLAND

D'APPOLONIA

524 286

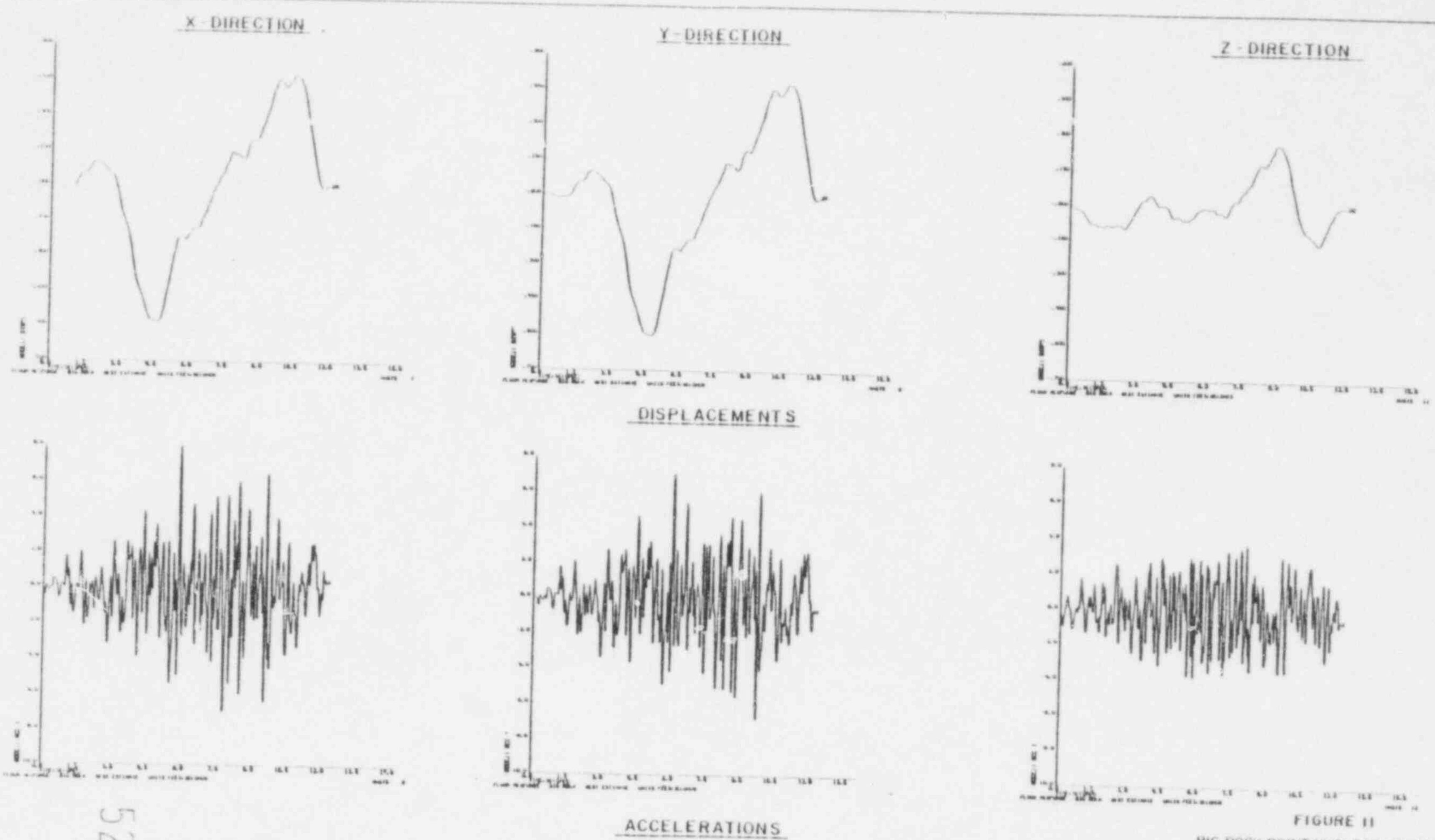

FIGURE 11

BIG ROCK POINT NUCLEAR POWER PLANT
FLOOR RESPONSES AT
SPENT FUEL POOL
LOCATION NODE 11

PREPARED FOR

NUS CORPORATION
ROCKVILLE, MARYLAND

D'APPOLONIA

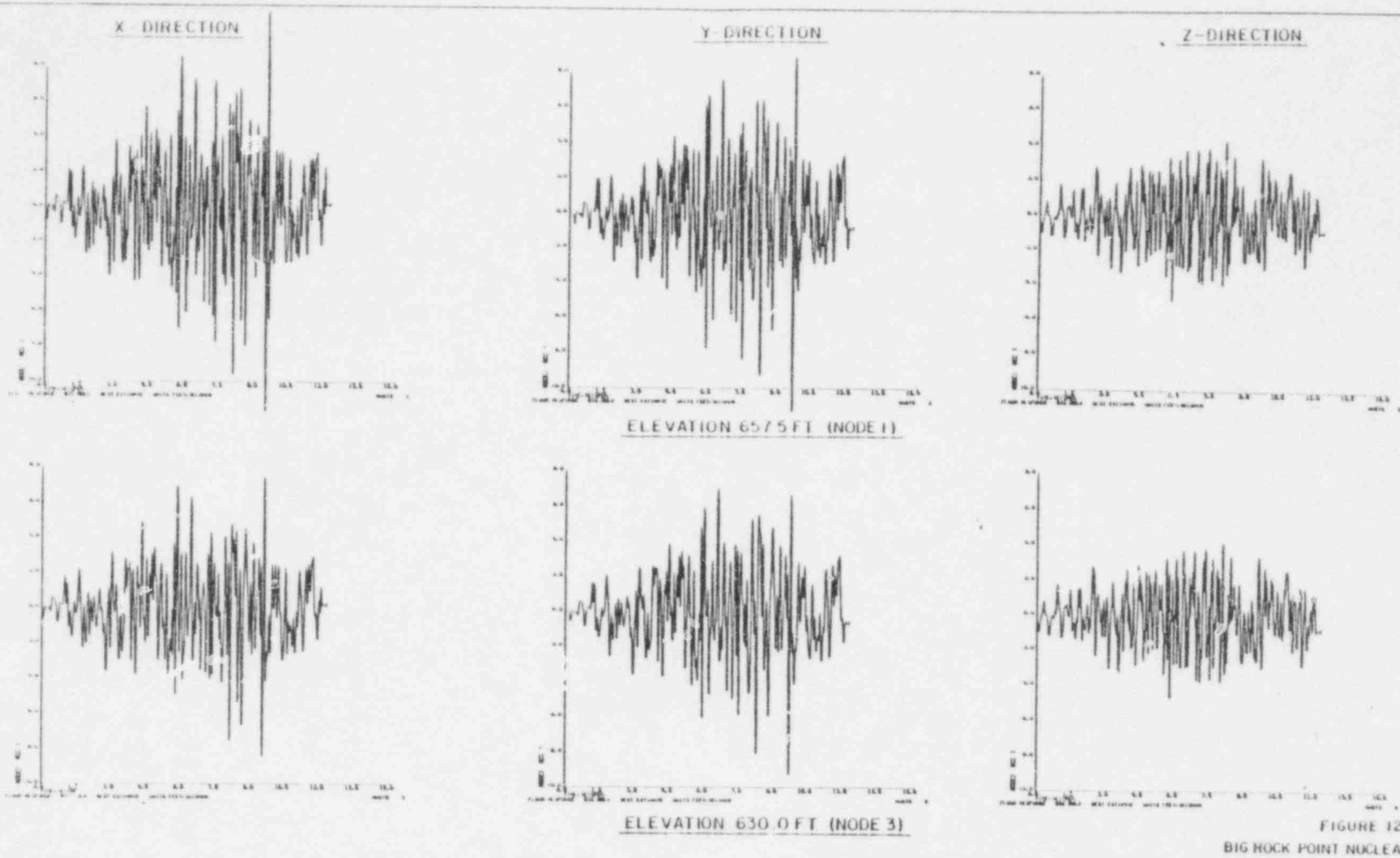

FIGURE 12

BIG ROCK POINT NUCLEAR POWER PLANT
FLOOR ACCELERATION RESPONSES
AT ELEVATION 657.5 FT (NODE 1)
AND ELEVATION 630.0 FT (NODE 3)

PREPARED FOR

NUS CORPORATION
ROCKVILLE, MARYLAND

D'APPOLONIA

DRAWN BY	CHECKED BY	APPROVED BY	DWG DRAWING NUMBER 78-161-B6

POOR ORIGINAL

524 288

DRAWN BY	FFW 6-13-78	CHECKED BY / APPROVED BY	SC / ADH	JUN 27 78 / 6/27/78	DRAWING NUMBER	78-161-A11

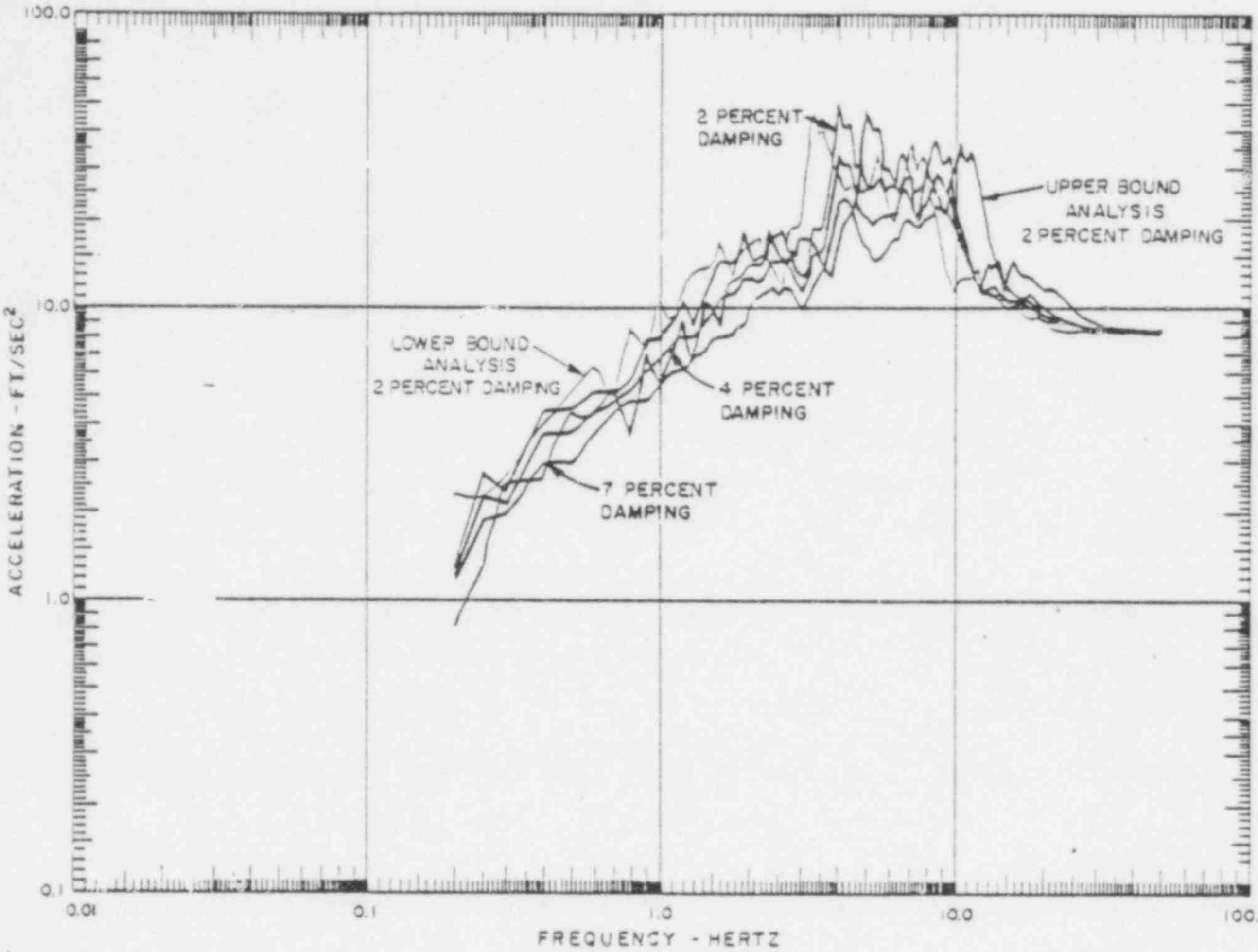

524 289

FIGURE 13

FLOOR RESPONSE SPECTRA
NODE 11-X DIRECTION
2, 4, AND 7 PERCENT DAMPING
PREPARED FOR

NUS CORPORATION
ROCKVILLE, MARYLAND

D'APPOLONIA

DRAWN BY	FFW 6-13-78	CHECKED BY / APPROVED BY	SC / ADH	JUN 27 78 / 6/27/78	DRAWING NUMBER	78-161-A12

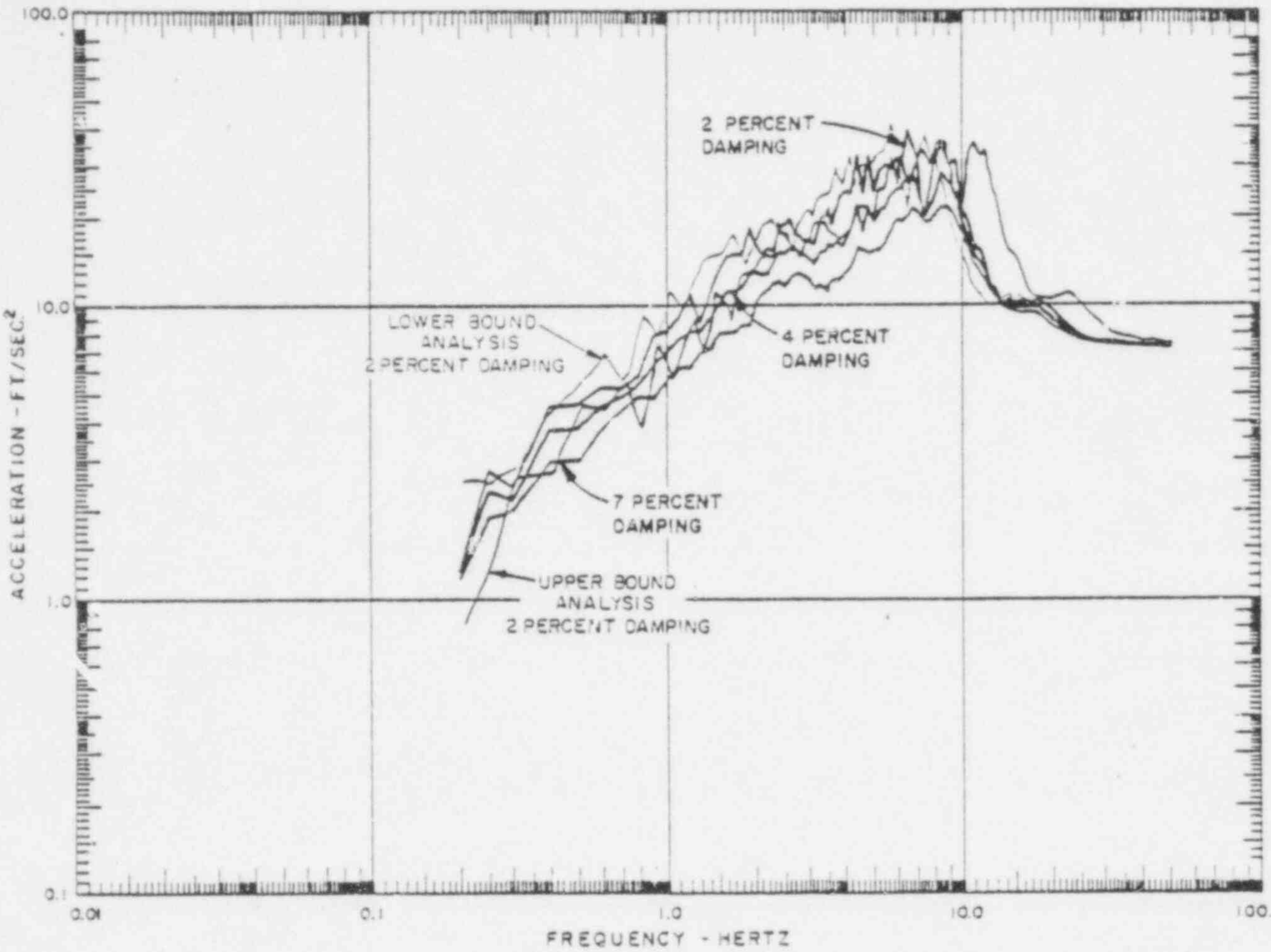

524 290

FIGURE 14

FLOOR RESPONSE SPECTRA
NODE 11 – Y DIRECTION
2, 4, AND 7 PERCENT DAMPING
PREPARED FOR

NUS CORPORATION
ROCKVILLE, MARYLAND

POOR ORIGINAL

D'APPOLONIA

DRAWN BY	FFW 6-13-78	CHECKED BY	SC 3JUN 27 78	DRAWING NUMBER	78-161-A13
		APPROVED BY	ADH 6/27/78		

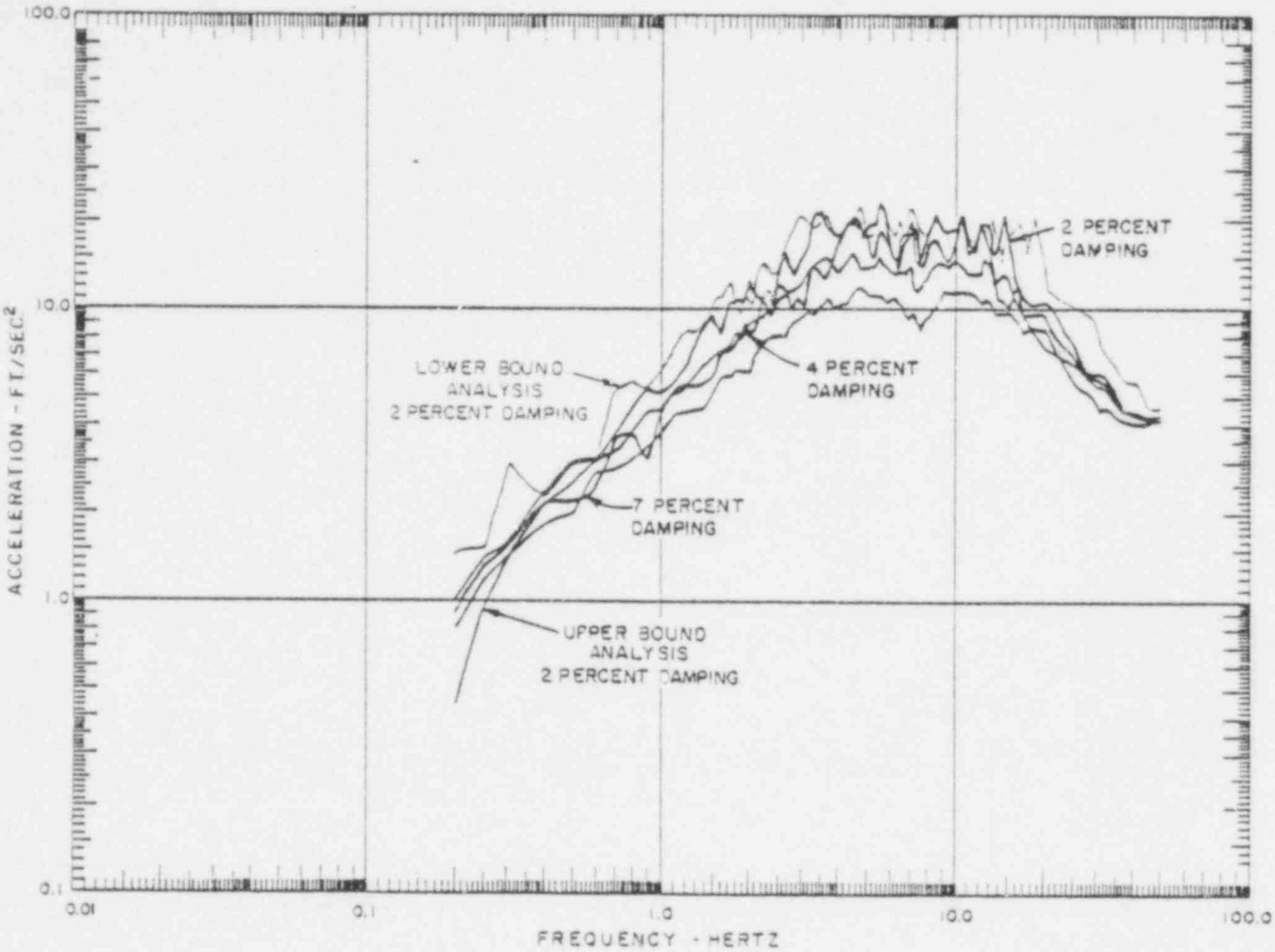

524 291

FIGURE 15

FLOOR RESPONSE SPECTRA
NODE 11 – Z DIRECTION
2, 4, AND 7 PERCENT DAMPING
PREPARED FOR

NUS CORPORATION
ROCKVILLE, MARYLAND

POOR ORIGINAL

D'APPOLONIA

DRAWN BY FFW 6-13-78 | CHECKED BY SC JUN 27 78 | APPROVED BY ADH 6/27/78 | DRAWING NUMBER 78-161-A6

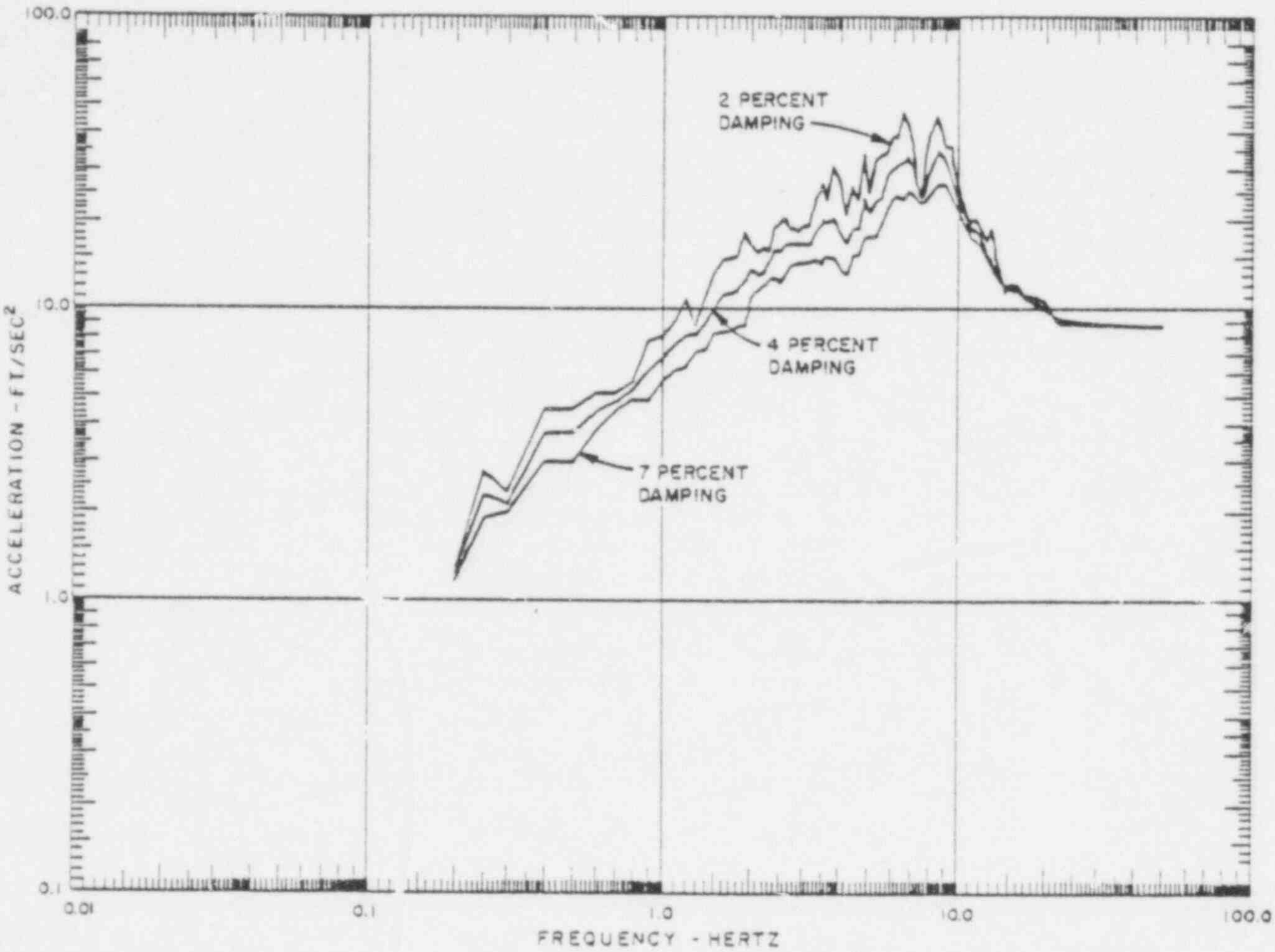

524 292

FIGURE 16

FLOOR RESPONSE SPECTRA
NODE 3 — X DIRECTION
2, 4, AND 7 PERCENT DAMPING
PREPARED FOR

NUS CORPORATION
ROCKVILLE, MARYLAND

POOR ORIGINAL

D'APPOLONIA

DRAWN BY	CHECKED BY	SC		DRAWING NUMBER
FFW 6-13-78	APPROVED BY	ADH	6/27/78	78-161-A7

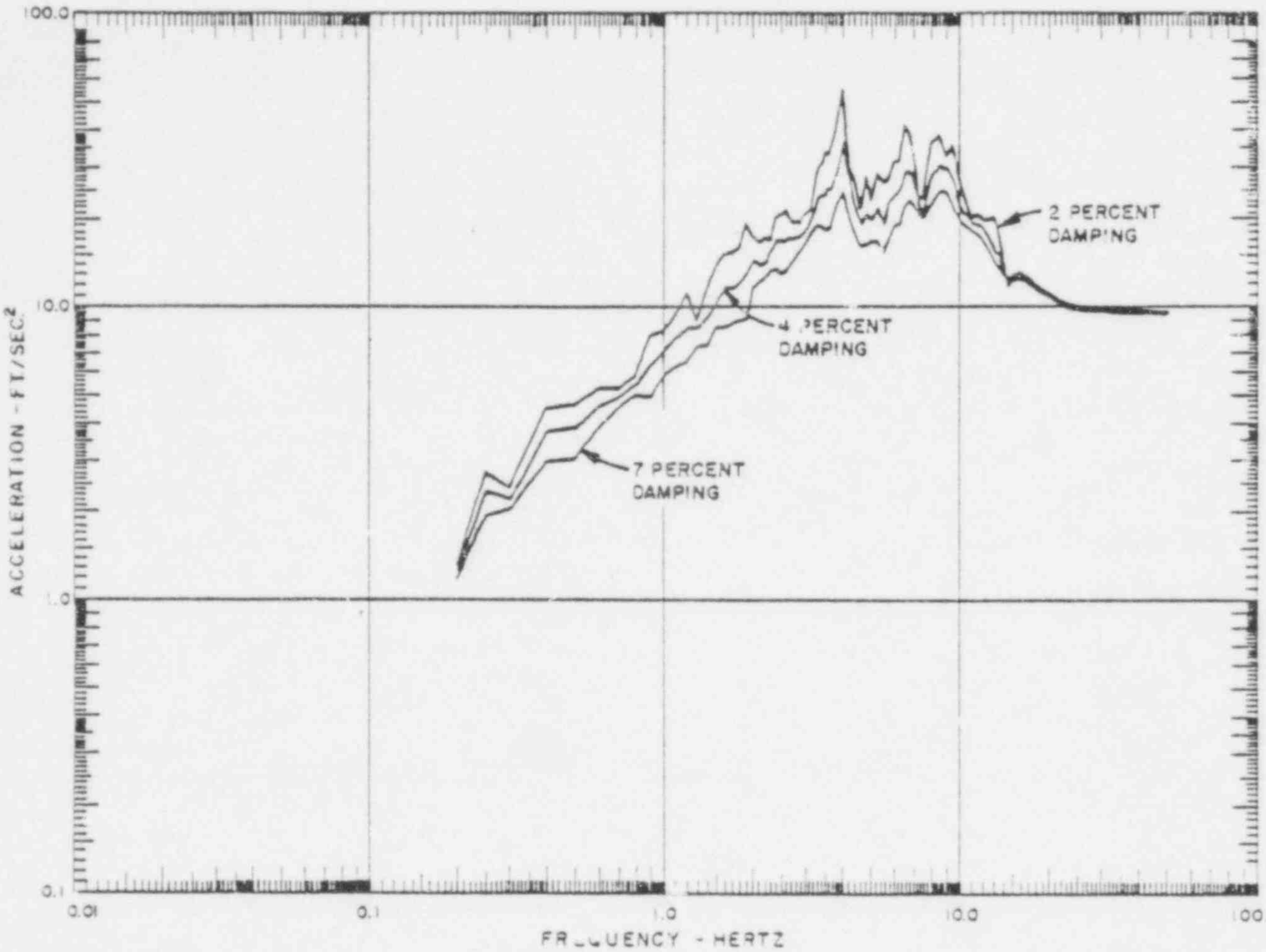

524 293

FIGURE 17

FLOOR RESPONSE SPECTRA
NODE 3 — Y DIRECTION
2, 4, AND 7 PERCENT DAMPING
PREPARED FOR

NUS CORPORATION
ROCKVILLE, MARYLAND

D'APPOLONIA

DRAWN BY	FFW 6-13-78	CHECKED BY APPROVED BY	SC ADH	JUN 27 78 6/27/78	DRAWING NUMBER	78-161-A5

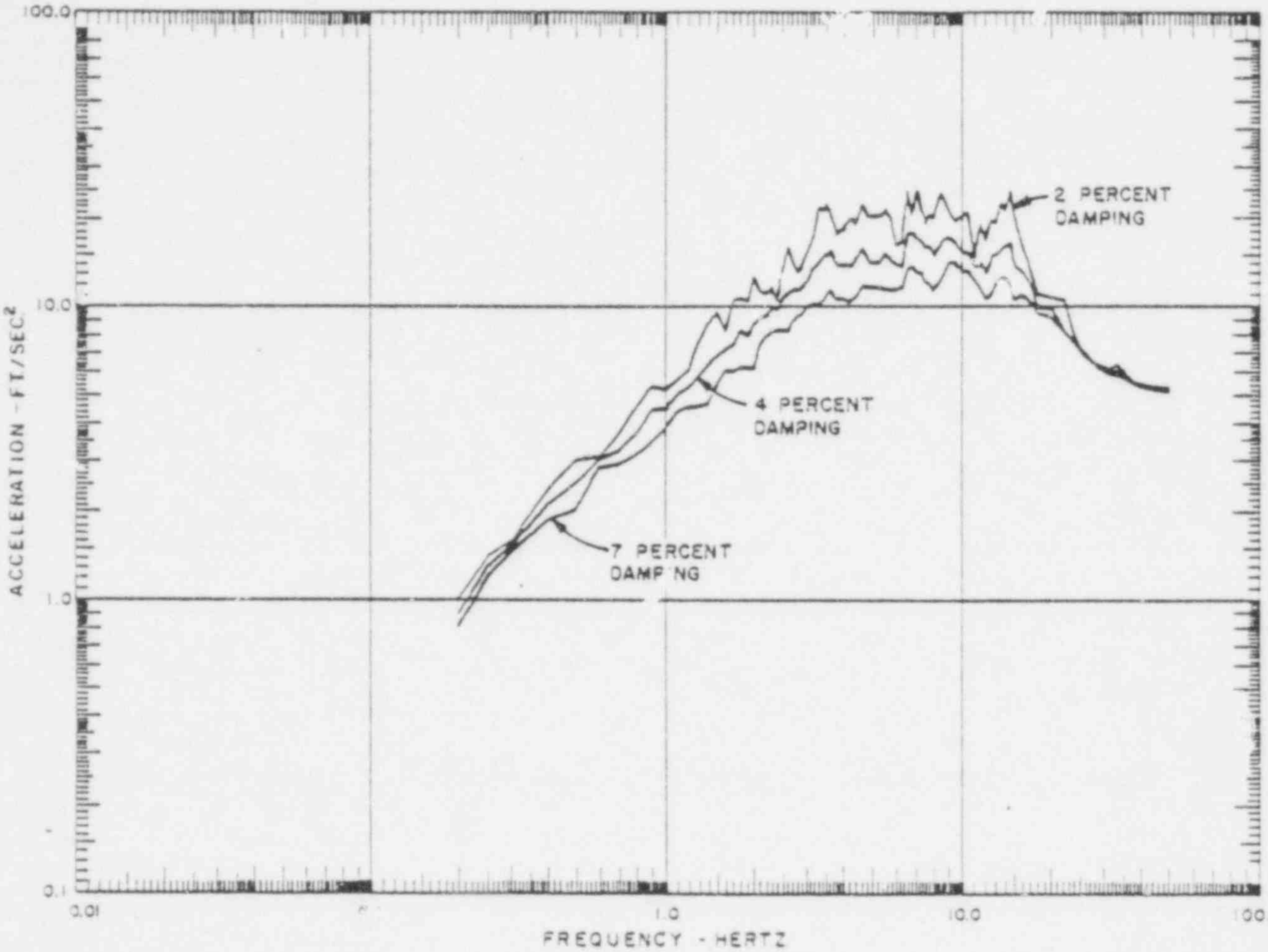

524 294

FIGURE 18

FLOOR RESPONSE SPECTRA
NODE 3 — Z DIRECTION
2, 4, AND 7 PERCENT DAMPING
PREPARED FOR

NUS CORPORATION
ROCKVILLE, MARYLAND

POOR ORIGINAL

D'APPOLONIA

DRAWN BY	FFW 6-13-78	CHECKED BY	SC	JUN 27 78	DRAWING NUMBER	78-161-A8
		APPROVED BY	ADH	6/27/78		

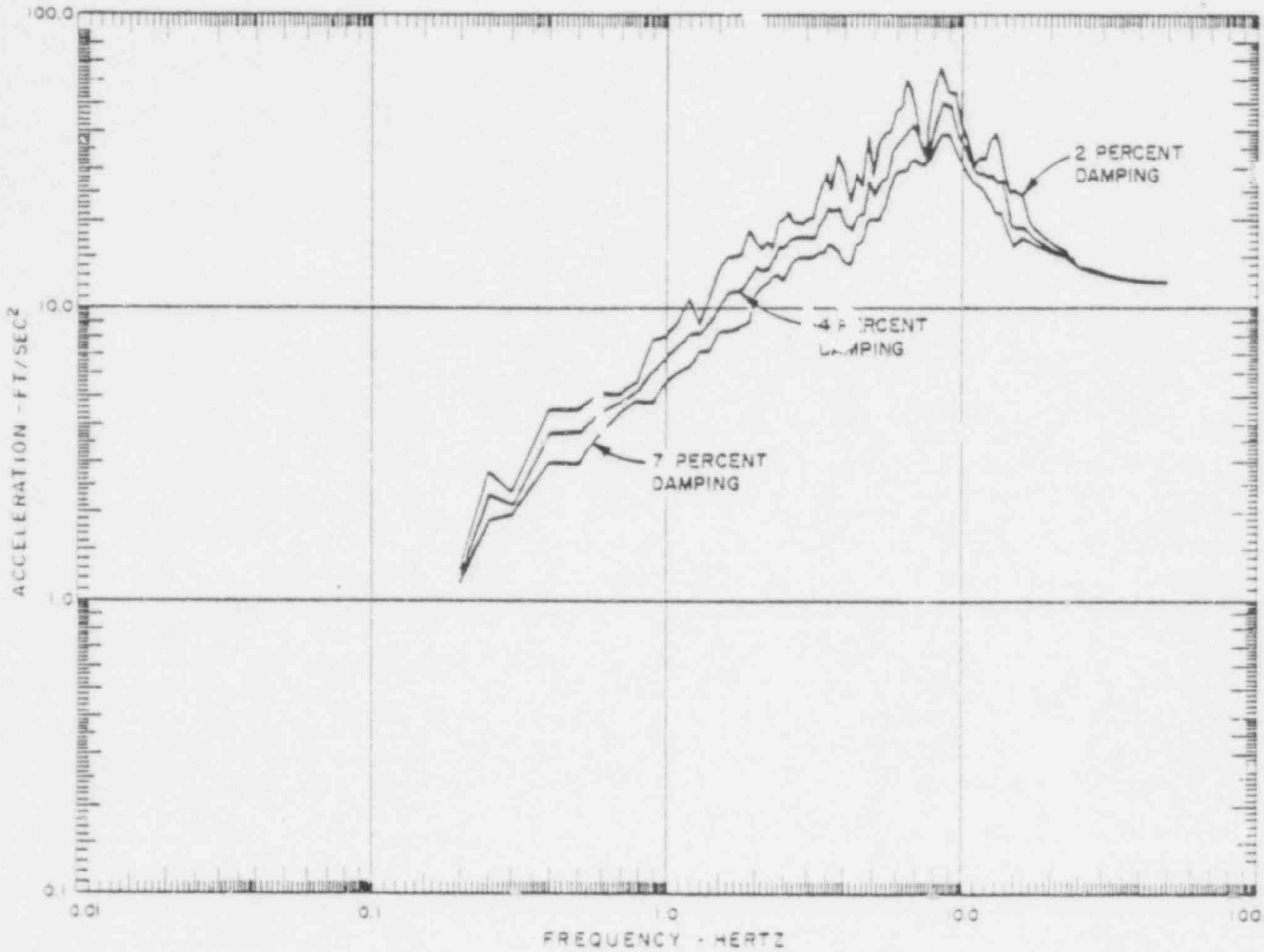

524 295

FIGURE 19

FLOOR RESPONSE SPECTRA
NODE I — X DIRECTION
2, 4, AND 7 PERCENT DAMPING
PREPARED FOR

NUS CORPORATION
ROCKVILLE, MARYLAND

POOR ORIGINAL

D'APPOLONIA

DRAWN BY	CHECKED BY	SC	JUN 27 78	DRAWING NUMBER
FFW 6-13-78	APPROVED BY	ADH	6/27/78	78-161-A9

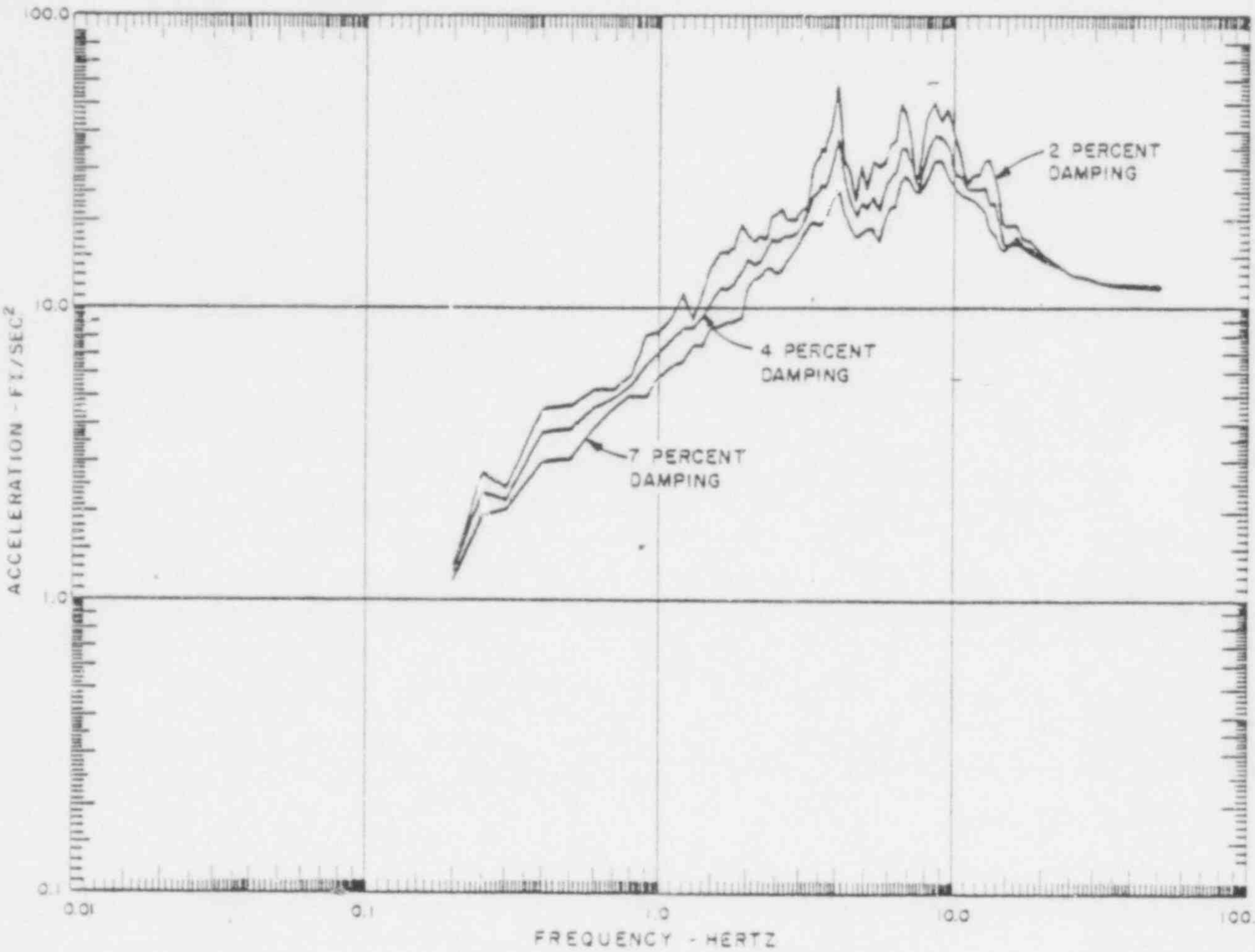

524 296

FIGURE 20

FLOOR RESPONSE SPECTRA
NODE I – Y DIRECTION
2, 4, AND 7 PERCENT DAMPING
PREPARED FOR

NUS CORPORATION
ROCKVILLE, MARYLAND

POOR ORIGINAL

D'APPOLONIA

DRAWN BY	FFW 6-13-78	CHECKED BY	9C JUN 27 78	DRAWING NUMBER	78-161-A10
		APPROVED BY	ADH 6/27/78		

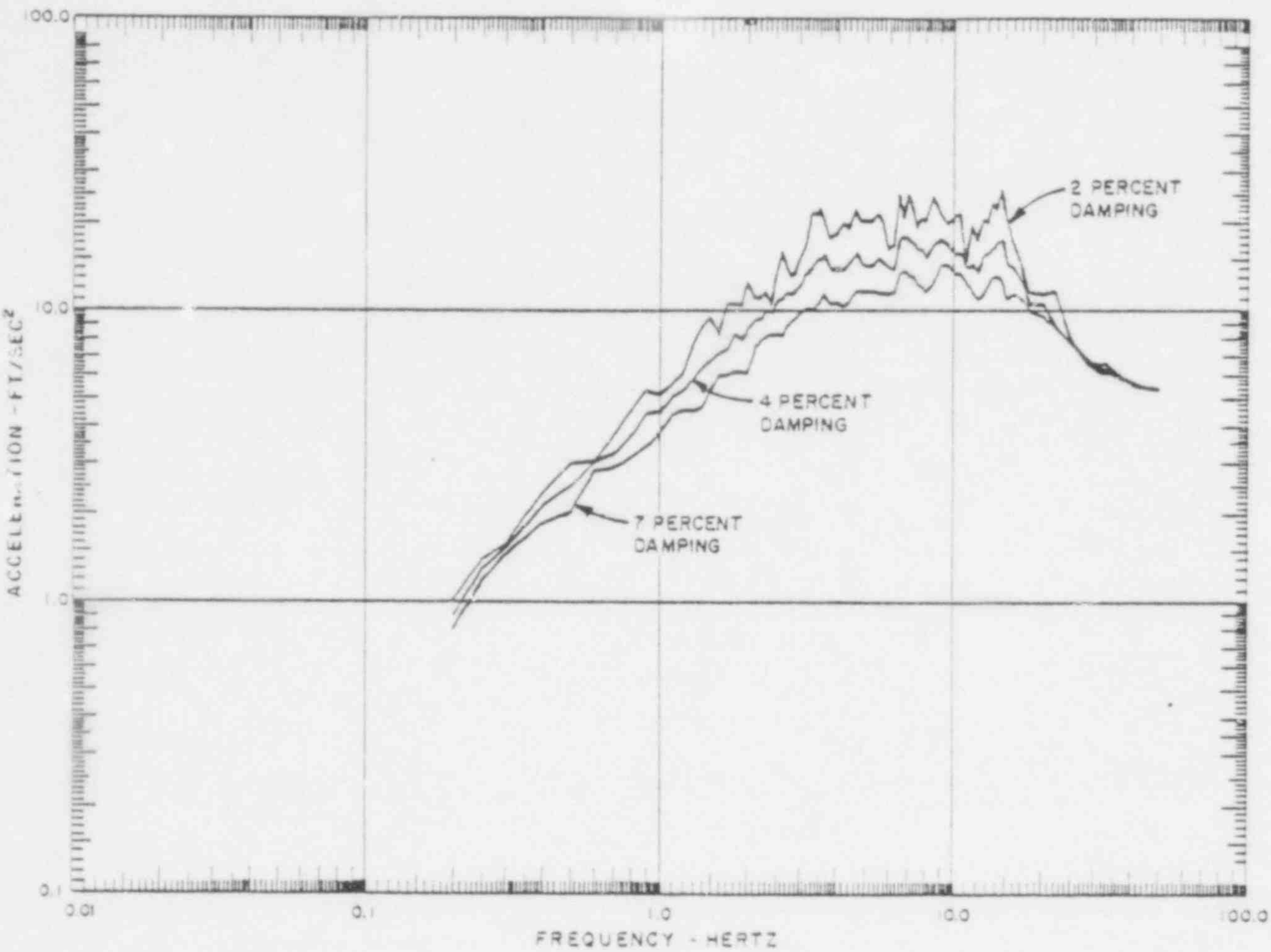

524 297

FIGURE 21

FLOOR RESPONSE SPECTRA
NODE 1 — Z DIRECTION
2, 4, AND 7 PERCENT DAMPING
PREPARED FOR

NUS CORPORATION
ROCKVILLE, MARYLAND

POOR ORIGINAL

D'APPOLONIA